MARKOV CHAIN APPROXIMATION OF ONE-DIMENSIONAL STICKY DIFFUSIONS

CHRISTIAN MEIER* AND
LINGFEI LI,* *The Chinese University of Hong Kong*
GONGQIU ZHANG,** *The Chinese University of Hong Kong, Shenzhen*

Abstract

We develop a continuous-time Markov chain (CTMC) approximation of one-dimensional diffusions with sticky boundary or interior points. Approximate solutions to the action of the Feynman–Kac operator associated with a sticky diffusion and first passage probabilities are obtained using matrix exponentials. We show how to compute matrix exponentials efficiently and prove that a carefully designed scheme achieves second-order convergence. We also propose a scheme based on CTMC approximation for the simulation of sticky diffusions, for which the Euler scheme may completely fail. The efficiency of our method and its advantages over alternative approaches are illustrated in the context of bond pricing in a sticky short-rate model for a low-interest environment and option pricing under a geometric Brownian motion price model with a sticky interior point.

Keywords: Diffusions; sticky boundary; Markov chain approximation; simulation; Sturm–Liouville problem

2010 Mathematics Subject Classification: Primary 65C40; 60J60; 65C05
Secondary 34L10; 34L16

1. Introduction

We consider a one-dimensional (1D) regular diffusion process X on an interval $\mathbb{S}$ with endpoints l and r, where a boundary point or an interior point is sticky. A point a is said to be sticky if the occupation time of the process at a, i.e.,

$$O_t^a(X) = \int_0^t I(X_s = a)\, d\langle X \rangle_s,$$

is positive for all $t > 0$ if $X_0 = a$ and $\langle X \rangle$ is the quadratic variation of X (see e.g. [28, Section 15.8] or [46, Chapter VI]). Sticky boundary behavior was first discovered by [18], and a historical account is given in [45]. The focus of this paper will be on the case of a single sticky point, although our method can be easily extended to handle the case of multiple sticky points.

Diffusion processes with sticky points have applications in various areas. For applications in physics and biology, see e.g. [5], [6], [20], [27], [44], and [54]. Sticky diffusions also arise as

the limiting process of time-changed random walks ([2]) and a class of storage models ([23], [53]). Recently, [42] proposed modeling short rates (i.e., instantaneous interest rates) by an Ornstein–Uhlenbeck (OU) diffusion with zero as the sticky lower bound (see also [43]). The author of [42] shows that this model is able to produce yield curves of various shapes observed in the market, in particular, the *S* shape that occurred after the 2008 financial crisis. Financial applications of geometric Brownian motions with a sticky interior point are discussed in [26].

There also exist a number of mathematical studies on sticky diffusions. The sticky Brownian motion is studied in [4], [16], and [51] with respect to the existence and uniqueness of weak and strong solutions. The paper [43] establishes the existence of a unique weak solution to the sticky OU stochastic differential equation (SDE). Some characterizations of more general sticky diffusions can be found in [25].

This paper is mainly concerned with the computation of general 1D sticky diffusions. For the sticky Brownian motion, its transition density is obtained in closed form in [13]. We are interested in calculating the action of the Feynman–Kac operator on a payoff function, which is required in many applications, as well as first passage probabilities. For the sticky OU model, [43] obtains semi-analytical solutions expressed as infinite series using the eigenfunction expansion method. The drawback of this approach is that approximating the infinite series can require many terms if the time horizon is not long enough, making it computationally inefficient. Furthermore, this method cannot be applied to general sticky diffusions as their eigenvalues and eigenfunctions are generally unavailable.

1.1. Summary of contributions

The contributions of the present paper are threefold. First of all, the main contribution is a novel, general, and efficient computational method based on continuous-time Markov chain (CTMC) approximation for sticky diffusions. We offer two constructions of a CTMC approximation and show that a carefully designed scheme achieves second-order convergence. We compare this scheme with a well-known finite difference scheme that numerically solves the parabolic partial differential equation (PDE) associated with the Feynman–Kac operator; our method is much faster for similar levels of accuracy. Another advantage of our method is that it is probabilistic, whereas the finite difference method is not. Its probabilistic nature allows us to also solve the simulation problem of 1D sticky diffusions, for which the widely used Euler discretization may fail completely because of its inability to simulate the sticky behavior at the boundary. Our solution is simply to simulate from the CTMC that approximates the sticky process. Although this method is biased, the bias can be properly contained, and a numerical experiment shows that the method yields accurate results.

The second contribution is on computing matrix exponentials, which is required in many CTMC-based algorithms. There exist well-known stable algorithms, such as the scaling and squaring algorithm of [24], but they may not be efficient enough. In this paper, we find that an extrapolation-based numerical ordinary differential equation (ODE) method from [19] works much better than standard algorithms for computing matrix exponentials in our problem. We recommend using it for computation of matrix exponentials, especially for long horizons.

Our third contribution is numerical analysis of approximations to an important type of Sturm–Liouville problem whose eigenparameter appears in the boundary condition. To the best of our knowledge, our estimates of the approximation errors for the eigenvalues and eigenfunctions are new, and thus we also contribute to the literature on Sturm–Liouville problems. Based on these estimates, we utilize the eigenfunction expansions of the exact and approximate solutions to obtain sharp estimates of the convergence rates of the two CTMC approximation schemes.

1.2. Comparison with existing literature

CTMC approximation has been developed for many types of diffusions and Markov jump processes to solve various types of problems, but not for sticky diffusions. See [9], [10], [11], [12], [17], [30], [40], [49], and [56], among others, for related literature on CTMC approximation for financial applications. In the following, we compare our paper with some closely related works.

(1) Analysis of the convergence rate of a CTMC approximation in the present paper is based on spectral representations, which are also used in [35] and [55]. However, there exist major differences in the analysis. The most important distinction is the boundary condition. The papers [35] and [55] deal with killing boundary behavior for diffusions, while this paper considers sticky boundary behavior. This change in boundary condition brings an additional term of point mass to the speed measure, which requires the proofs of many results to be either adapted (e.g., Proposition 1 and Theorem 4) or done using new ideas (e.g., Lemma 2, Propositions 2, 3, and 4, and Theorem 3).

(2) After the initial submission of this paper, we learned about [8], which develops CTMC approximation for a Brownian motion with a lower sticky boundary and also uses it to simulate this sticky process. However, the two papers have some major differences. First, [8] considers only a sticky Brownian motion, whereas our paper deals with general diffusions. Second, in [8] the CTMC is restricted to live on a uniform grid, while our paper allows the CTMC to live on a general non-uniform grid. This may be useful in applications with non-smooth payoffs. Third, to obtain the convergence rate of a CTMC approximation, [8] directly assumes the smoothness of the value function. This, however, may be difficult to check in advance. In contrast, our convergence rate analysis does not make any prior assumption on the smoothness of the value function. In fact, we deduce its smoothness from the spectral representation and the properties of the eigenvalues and eigenfunctions.

(3) The paper [3] approximates general diffusions with sticky interior and boundary points by interpolated discrete-time Markov chains. The method of [3] requires time-discretization, whereas our method does not discretize time in constructing the Markov chain. A further difference is that [3] shows that its approximation converges at fixed times with rate 1/4 in terms of the Wasserstein distance, which measures the discrepancy between the path distribution of a diffusion and its corresponding Markov chain approximation. By contrast, we use the maximum norm to measure the approximation error for quantities of interest.

Our discussions in this paper are mainly focused on the case of a sticky lower boundary, but we will also address the case of a sticky interior point in some detail. The rest of the paper is organized as follows. Section 2 provides various characterizations of 1D diffusions with a sticky lower boundary. We first give a general set of conditions that implies the existence of a unique solution to the sticky SDE. Then we define the Feynman–Kac semigroup of the sticky process, derive its infinitesimal generator, and obtain its eigenfunction expansion. In Section 3, we construct two CTMC approximation schemes for the sticky diffusion and show how to calculate the quantities of interest under the CTMC. We show that the generator of the CTMC also admits an eigenfunction expansion, which will be employed for the convergence rate analysis. Section 4 derives the convergence rate. Section 5 contains various numerical results on the pricing of zero-coupon bonds under the sticky OU model of [43], and of European call options under the geometric Brownian motion model with a sticky interior point from [26]. Section 6 summarizes the paper and discusses future research. The proofs of the major results are collected in the appendix. In the online supplement, we provide additional proofs and pseudocode for our method.

2. Characterizations of 1D diffusions with a lower sticky boundary

The sticky diffusion under analysis will be defined as a weak solution to the following system of SDEs:

$$dX_t = \mu\,(X_t)\,I\,(X_t > l)\,dt + \sigma\,(X_t)\,I\,(X_t > l)\,dB_t + \frac{1}{2}dL_t^l\,(X)\,, \qquad (2.1)$$

$$I\,(X_t = l)\,dt = \frac{1}{2\rho}dL_t^l\,(X)\,, \qquad (2.2)$$

where $\rho \in (0, \infty)$ represents the stickiness of X_t at l, I is the indicator function, and L_t^l is the (right) local time process of X at l, defined as

$$L_t^l\,(X) := \lim_{\varepsilon \searrow 0} \frac{1}{\varepsilon} \int_0^t I\,(X_s \in [l, l+\varepsilon])\,d\langle X \rangle_s \quad \text{in probability.}$$

A weak solution to the above system of SDEs is a pair of adapted processes (X, B) defined on a filtered probability space $(\Omega, \mathcal{F}, (\mathcal{F}_t)_{t\geq 0}, \mathbb{P})$ where B is a standard Brownian motion and both equations are satisfied. Uniqueness in law holds if for any two solutions (X, B) and (X^1, B^1), X and X^1 have the same law. We will say that joint uniqueness in law holds if for the two solutions, the pairs (X, B) and (X^1, B^1) have the same law.

We will first provide a set of conditions for the existence of a unique weak solution in law. Notice that two other types of boundary behavior can be recovered from the sticky case as limits. If $\rho = 0$, l becomes an absorbing boundary and if $\rho = \infty$, the process is instantaneously reflected at l. We adopt the method of time change that constructs the sticky diffusion process as a time-changed reflected diffusion process with the same drift and diffusion coefficient in the interior of the state space.

2.1. Existence and uniqueness of weak solutions

We make the following assumption.

Assumption 1. *Assume that for the given drift and volatility coefficients, there exists a unique weak solution to (2.1) and (2.2) in the case of $\rho = \infty$ (i.e., l is a reflecting boundary). Furthermore, suppose $\sigma^2(x) > 0$ for all $x \in \mathbb{S}$.*

The well-posedness of reflected SDEs has been well studied, and conditions can be found in, e.g., [37], [47], [48], [50], and [52]. Let X^1 denote the diffusion instantaneously reflected at l. We apply the time change

$$T_t = \left(t + \frac{1}{2\rho}L_t^l(X^1)\right)^{-1}$$

to X^1, which slows it down whenever it hits l. This introduces stickiness, which can be thought of as slow reflection. This construction enables us to show that there exists a unique weak solution to the sticky SDE system as long as this is so for the reflecting case.

Theorem 1. *Under Assumption 1, Equations (2.1) and (2.2) have a jointly unique weak solution for any $\rho \in (0, \infty)$.*

The proof of this theorem can be found in the online supplement; it is similar to the proof of [42, Theorem 4.1]. We follow the standard approach to study the diffusion process with reflecting boundary condition and apply a time change to slow down the movement into the

interior, which creates stickiness. However, the fact that the time change is continuous and strictly increasing is shown differently, as the arguments in [42] are only valid for the OU process and cannot be applied to general diffusions.

The following theorem shows that it is possible to add the local time given in (2.2) as an additional term in the drift.

Theorem 2. *If $\rho \in (0, \infty)$, then (2.1) and (2.2) are equivalent to the following SDE:*

$$dX_t = \mu (X_t) I (X_t > l) dt + \rho I (X_t = l) dt + \sigma (X_t) I (X_t > l) dB_t. \tag{2.3}$$

Furthermore, X is a strong Markov process.

The proof of this theorem is omitted, as it is similar to that of Theorem 4.1 and Corollary 4.3 in [42]. Theorem 1 and Theorem 2 together show that X is a diffusion process. Its stickiness at l is measured by ρ; the smaller the value of ρ, the more X sticks to l.

2.2. Feynman–Kac semigroup and infinitesimal generator

The Feynman–Kac operator $\mathcal{P}_t$ associated with the diffusion X is defined by

$$\mathcal{P}_t f(x) := \mathbb{E}_x \Big(\exp \Big(- \int_0^t k (X_u) \, du \Big) f (X_t) \Big), \qquad x \in \mathbb{S}, \tag{2.4}$$

where the function k is assumed to be nonnegative. We can interpret k as the discount factor and f as the payoff function. Let $u(t, x) = \mathcal{P}_t f(x)$; this is called the value function. Financially, $u(t, x)$ is the price for receiving payoff f at t given the current state x. The semigroup $(\mathcal{P}_t)_{t \geq 0}$ is a strongly continuous contraction semigroup on $B_b(\mathbb{S})$, the space of bounded Borel-measurable functions, endowed with the maximum norm.

Assume that μ, σ, and k are continuous over $\mathbb{S}$. Using the arguments in [42], one can easily show that the infinitesimal generator $\mathcal{G}$ of $(\mathcal{P}_t)_{t \geq 0}$ acts on

$$\mathcal{D} := \Big\{ f \in C^2(\mathbb{S}) \cap C_b(\mathbb{S}) : \mathcal{G}f \in C_b (\mathbb{S}) , \ \mu (l) f' (l) + \frac{1}{2}\sigma^2 (l) f'' (l) = \rho f' (l) \Big\}$$

as follows:

$$\mathcal{G}f(x) = (\mu(x)I (x > l) + \rho I (x = l)) f'(x) + \frac{1}{2}\sigma^2(x)I (x > l) f''(x) - k(x)f(x). \tag{2.5}$$

In particular, for $f \in \mathcal{D}$,

$$\mathcal{G}f (l) = \rho f' (l) - k (l) f (l) . \tag{2.6}$$

Remark 1. The Feynman–Kac semigroup can also be seen as the transition semigroup of a process $\tilde{X}$ which is killed at rate k; i.e., $\tilde{X}$ has the same drift and diffusion coefficients as X but is killed at its lifetime $\tilde{\zeta} = \inf\{t \geq 0 : \int_0^t k(X_u)du \geq e\}$, where $e \sim \text{Exp}(1)$ is exponentially distributed with rate 1. At the lifetime $\tilde{\zeta}$ the process is sent to the cemetery state. It can be proved that

$$\mathcal{P}_t f(x) = \mathbb{E}_x \Big(f(\tilde{X}_t)I(\tilde{\zeta} > t) \Big). \tag{2.7}$$

See e.g. [36, Section 1.1] for a detailed explanation.

We can write

$$\mathcal{P}_t f(x) = \int_{\mathbb{S}} P (t, x, dy) f (y) ,$$

where $P(t, x, \cdot)$ is the transition probability measure of the process on $\mathbb{S}$. It has a point mass at l and a density on $\mathbb{S} \setminus \{l\}$, denoted by $p(t, x, \cdot)$. We can further write

$$\mathcal{P}_t f(x) = P(t, x, l) f(l) + \int_{\mathbb{S}} p(t, x, y) f(y)\, dy. \tag{2.8}$$

Note that we simply write $P(t, x, l)$ for $P(t, x, \{l\})$.

2.3. Eigenfunction expansion representations

Let S and M be the scale and speed measure of X. Using the results in [7, Section II], we can obtain that the scale measure has a density, i.e., $S(dx) = s(x)dx$ with

$$s(x) = \exp\left(-\int_l^x \frac{2\mu(y)}{\sigma^2(y)}dy\right),$$

and the speed measure is of a mixed type, with

$$M(dx) = m(x)dx + \frac{1}{\rho}\delta_l(dx) = \frac{2}{\sigma^2(x)s(x)}dx + \frac{1}{\rho}\delta_l(dx),$$

where δ_l is the Dirac delta measure at l. In future discussions, we will use $M(l)$ instead of $M(\{l\})$ to simplify the notation.

It is possible to extend $(\mathcal{P}_t)_{t \geq 0}$ to a self-adjoint semigroup on the Hilbert space $L^2(\mathbb{S}, M)$ of square-integrable functions on $\mathbb{S}$ with respect to M. The inner product in this space is

$$(f, g) = \int_{\mathbb{S}} f(x)g(x)M(dx) = \frac{1}{\rho}f(l)\,g(l) + \int_{\mathbb{S}^\circ} \frac{2f(x)g(x)}{\sigma^2(x)s(x)}dx.$$

The application of spectral methods to study diffusions dates back to [38]. When the spectrum of the generator of the diffusion is simple and purely discrete, a general spectral expansion reduces to an eigenfunction expansion. We make the following assumption for the existence of an eigenfunction expansion.

Assumption 2. *The right boundary r is finite, and X is sent to the cemetery state ∂ once it reaches r. Suppose that μ and σ satisfy the requirements in Assumption 1. Furthermore, suppose that $\mu \in C^3(\mathbb{S})$, $\sigma^2 \in C^4(\mathbb{S})$, and $k \in C^2(\mathbb{S})$ with $k(x) \geq 0$ for all $x \in \mathbb{S}$.*

Under Assumption 2, X lives on $\mathbb{S} = [l, r) \cup \{\partial\}$, and we extend the definition of k and the payoff function f to ∂ by setting $k(\partial) = f(\partial) = 0$ in (2.4). Theorem 3.2 in [36] shows that the spectrum of $\mathcal{G}$ is purely discrete and simple, and we have the following eigenfunction expansions:

$$P(t, x, l) = M(l) \sum_{k=1}^{\infty} \exp(-\lambda_k t)\, \varphi_k(x)\varphi_k(l) \qquad \text{for } x \in \mathbb{S}, \ t > 0, \tag{2.9}$$

$$p(t, x, y) = m(y) \sum_{k=1}^{\infty} \exp(-\lambda_k t)\, \varphi_k(x)\varphi_k(y) \qquad \text{for } x, y \in \mathbb{S}, \ y \neq l, \ t > 0, \tag{2.10}$$

$$u(t, x) = \sum_{k=1}^{\infty} (f, \varphi_k) \exp(-\lambda_k t)\, \varphi_k(x) \qquad \text{for } f \in L^2(\mathbb{S}, M), \ x \in \mathbb{S}, \ t > 0,$$

where (λ_k, φ_k) is the kth eigenpair which solves the Sturm–Liouville problem

$$
\begin{aligned}
\mathcal{G}\varphi(x) &= -\lambda\varphi(x) && \text{for all } x \in \mathbb{S}^{\circ}, \\
\rho\varphi'(l) - (k(l) - \lambda)\,\varphi(l) &= 0 && \varphi(r) = 0.
\end{aligned}
\tag{2.11}
$$

The eigenfunctions satisfy $\int_l^r \varphi_i(x)\varphi_j(x)M(dx) = \delta_{ij}$ (here δ_{ij} is the Kronecker delta), and hence the solutions of (2.11) form a complete orthonormal basis of $L^2(\mathbb{S}, M)$.

Remark 2. Notice that Assumption 2 is not necessary for the spectrum to be purely discrete. For some sticky diffusions with infinity as the right boundary, such as the sticky OU process, and for sticky diffusions with other types of boundary behavior at finite r, the spectrum is also purely discrete and hence there exist eigenfunction expansions. We make Assumption 2 for two reasons. First, in our computational method, we need to localize the infinite right boundary to a large finite value to construct a CTMC, so it makes sense to assume the sticky diffusion under analysis has a finite right boundary. The error caused by localization is typically very small. Second, assuming that r is a killing boundary leads to the Dirichlet condition for the Sturm–Liouville problem at r. This is the only type of boundary condition for r that we will analyze in this paper, although other types of boundary conditions (e.g., Neumann) can also be handled using our method.

The eigenfunction expansion method has been extensively applied in finance for derivatives pricing. See for example [14], [31], [32], [33], and [36], among many others. The Sturm–Liouville problem associated with the sticky diffusion is different from those studied in the cited papers in that the eigenparameter also appears in the boundary condition, which makes the problem more difficult. The following proposition provides the asymptotic behavior of the eigenvalues and eigenfunctions of this type of Sturm–Liouville problem.

Proposition 1. *Under Assumption 2, there exist constants $C_1, C_2, C_3 > 0$ such that for $k = 1, 2, \ldots,$*

$$
C_1 k^2 \le \lambda_k \le C_2 k^2,
\tag{2.12}
$$

$$
\left\| \varphi_k^{(i)} \right\|_{\infty} \le C_3 k^i, \qquad \text{for } i = 0, 1, \ldots, 4.
\tag{2.13}
$$

Here $\varphi_k^{(i)}(x)$ is the ith-order derivative of $\varphi_k(x)$, and $\varphi_k^{(0)}(x) = \varphi_k(x)$.

This result is proved by transforming the problem into the Liouville normal form and using the existing results in [1]. These results help to establish the bounds on the eigenvalues, which are then used to bound the norms of the eigenfunctions of the transformed problem. Finally, the bounds are preserved after transforming the problem back to its original formulation.

3. Continuous-time Markov chain approximation

This section develops a general method to compute (2.4) using CTMC approximation. Note that the Feynman–Kac semigroup of X is the transition semigroup of $\tilde{X}$, killed at rate k. In the following, we construct a CTMC denoted by Y to imitate the transition behavior of $\tilde{X}$. The CTMC lives on a generally non-uniform grid $\mathbb{S}_n = \{x_0, x_1, \ldots, x_n, x_{n+1}\}$ with $x_0 = l$ and $x_{n+1} = r$, and $\mathbb{S}_n^{\circ} = \{x_1, \ldots, x_n\}$ is the grid on $\mathbb{S}^{\circ} = (l, r)$. We also put $\partial\mathbb{S}_n = \{x_0, x_{n+1}\}$, $\mathbb{S}_n^{-} = \{x_0\} \cup \mathbb{S}_n^{\circ}$, and $\mathbb{S}_n^{+} = \mathbb{S}_n^{\circ} \cup \{x_{n+1}\}$. Define

$$
x^- = \operatorname*{argmax}_{y < x, y \in \mathbb{S}_n} |y - x|, \qquad x^+ = \operatorname*{argmin}_{y > x, y \in \mathbb{S}_n} |y - x|,
$$

for $x \in \mathbb{S}_n$. Then x^- is the grid point to the left of x and x^+ is the point to the right. We define $x_0^- = x_0$ and $x_{n+1}^+ = x_{n+1}$. Since the grid can be non-uniform, we must distinguish between the distances to grid points on the left and right. Let

$$\delta^+ x = x^+ - x, \quad \delta^- x = x - x^-, \quad \delta x = \frac{1}{2}\left(\delta^+ x + \delta^- x\right);$$

these are the right, left, and average grid size at a point x. The mesh size is denoted by $h_n = \max_{x \in \mathbb{S}_n^-} \delta^+ x$.

3.1. Transition rates of the CTMC

To obtain the transition rates of the CTMC that resembles the sticky diffusion $\tilde{X}$, we apply finite differences to discretize its generator given by (2.5) and (2.6). Introduce the following difference operators acting on a general function g:

$$\nabla^+ g(x) = \frac{g\left(x^+\right) - g(x)}{x^+ - x}, \qquad\qquad \nabla^- g(x) = \frac{g(x) - g\left(x^-\right)}{x - x^-},$$

$$\nabla g(x) = \frac{\delta^- x}{2\delta x}\nabla^+ g(x) + \frac{\delta^+ x}{2\delta x}\nabla^- g(x), \qquad \Delta g(x) = \frac{1}{\delta x}\left(\nabla^+ g(x) - \nabla^- g(x)\right).$$

For $x \in \mathbb{S}_n^\circ$, we approximate $\mathcal{G}g(x)$ for $g \in \mathcal{D}$ by approximating g' by ∇g and g'' by Δg, which gives us

$$G_n g(x) = \mu(x)\nabla g(x) + \frac{1}{2}\sigma^2(x)\Delta g(x) - k(x)g(x), \qquad \text{for } x \in \mathbb{S}_n^\circ. \qquad (3.1)$$

For $\mathcal{G}g(x_0)$, we apply $\nabla^+ g(x_0)$ to approximate $g'(x_0)$ and obtain

$$G_n g(x_0) = \rho\nabla^+ g(x_0) - k(x_0)g(x_0).$$

We specify x_{n+1} to be a killing boundary for the CTMC; i.e., the chain is sent to the cemetery state ∂ once it reaches x_{n+1}. So the state space of the chain is $\{x_0, \cdots, x_n, \partial\}$. Let $\mathbb{G}_n$ be an $(n+1) \times (n+1)$ matrix for the transition rates among the states $\{x_0, \cdots, x_n\}$. Then, based on the expression for G_n,

$$\mathbb{G}_n = \begin{pmatrix} -\frac{\rho}{\delta^+ x_0} - k(x_0) & \frac{\rho}{\delta^+ x_0} & 0 & \cdots \\ \mathbb{G}_{n,1,0} & -\mathbb{G}_{n,1,0} - \mathbb{G}_{n,1,2} - k(x_1) & \mathbb{G}_{n,1,2} & \cdots \\ 0 & \mathbb{G}_{n,2,1} & -\mathbb{G}_{n,2,1} - \mathbb{G}_{n,2,3} - k(x_2) & \cdots \\ \vdots & \vdots & \vdots & \ddots \end{pmatrix},$$

(3.2)

which is a tridiagonal matrix, and

$$\mathbb{G}_{n,i,i-1} = \frac{-\mu(x_i)\delta^+ x_i + \sigma^2(x_i)}{2\delta^- x_i \delta x_i}, \qquad i = 1, \ldots, n,$$

$$\mathbb{G}_{n,i,i+1} = \frac{\mu(x_i)\delta^- x_i + \sigma^2(x_i)}{2\delta^+ x_i \delta x_i}, \qquad i = 1, \ldots, n-1,$$

$$\mathbb{G}_{n,0,1} = \frac{\rho}{\delta^+ x_0}.$$

Note that in our calculation of (2.4) we do not need the transition rates involving ∂. We refer to this construction of $\mathbb{G}_n$ in (3.2) as Scheme 1.

It turns out that Scheme 1 only converges at first order. Below we provide a better scheme that improves approximation for the sticky behavior. In Scheme 2, we try to match the expectation and variance of the sticky diffusion in a short time, given that it starts from x_0, with those of the CTMC. Let $\hat{O}_t^{x_0}$ approximate the occupation time of $\tilde{X}$ at the left boundary $l = x_0$ up to time t, where t is understood to be very small. Then, after ignoring terms of higher order in t, we have the system of equations

$$\mathbb{G}_{n,0,1}\delta^+x_0 t = \mu(x_0)\left(t - \hat{O}_t^{x_0}\right) + \rho\hat{O}_t^{x_0}, \tag{3.3}$$

$$\mathbb{G}_{n,0,1}\left(\delta^+x_0\right)^2 t = \sigma^2(x_0)\left(t - \hat{O}_t^{x_0}\right), \tag{3.4}$$

together with the condition that $\mathbb{G}_{n,0,0} + \mathbb{G}_{n,0,1} + k(x_0) = 0$. Equation (3.3) matches the expected change from x_0 in t. The left-hand side is clearly the quantity for the CTMC, ignoring higher-order terms in t. The right-hand side can be explained as follows. Up to time t, the diffusion $\tilde{X}$ spent a length of time $\hat{O}_t^{x_0}$ at the boundary x_0 with drift ρ and a length of time $t - \hat{O}_t^{x_0}$ near x_0 with drift approximately equal to $\mu(x_0)$. Adding these up gives the right-hand side of (3.3). Equation (3.4) can be interpreted in an analogous way by noting that the change of $\tilde{X}$ does not have any variance while it is on the boundary.

Solving the above equations gives the following result:

$$\mathbb{G}_{n,0,1} = \frac{\rho}{\delta^+x_0 + \frac{\rho - \mu(x_0)}{\sigma^2(x_0)}\left(\delta^+x_0\right)^2}, \qquad \mathbb{G}_{n,0,0} = -\mathbb{G}_{n,0,1} - k(x_0),$$

$$\hat{O}_t^{x_0} = \frac{\sigma^2(x_0) - \mu(x_0)\delta^+x_0}{\sigma^2(x_0) + (\rho - \mu(x_0))\delta^+x_0}t.$$

The above expression shows that $t - \hat{O}_t^{x_0} = O(\delta^+x_0)$. Ignoring this difference in (3.3) yields the formula of $\mathbb{G}_{n,0,1}$ under Scheme 1. Now it is intuitively clear that Scheme 2 is better than Scheme 1, as it matches the first two moments, while Scheme 1 only cares about the first moment. In Section 4, we will prove that Scheme 2 achieves second-order convergence.

The operator G_n acting on $g(x_0)$ can be written in a unified way for both schemes as follows:

$$G_n g(x_0) = \rho\beta\nabla^+ g(x_0) - k(x_0) g(x_0),$$

where

$$\beta = \begin{cases} 1, & \text{Scheme 1,} \\ \frac{1}{1 + \frac{\rho - \mu(x_0)}{\sigma^2(x_0)}\delta^+x_0}, & \text{Scheme 2.} \end{cases} \tag{3.5}$$

Remark 3. Using Scheme 2 we can obtain CTMC approximation for the absorbing and instantaneous reflecting cases. If we set $\rho = 0$, then $\mathbb{G}_{n,0,1} = 0$ and $\hat{O}_t^{x_0} = t$, which shows the chain is absorbed at x_0. If we let $\rho \to \infty$, then $\mathbb{G}_{n,0,1} \to \sigma^2(x_0)/(\delta^+x_0)^2$ and $\hat{O}_t^{x_0} \to 0$. This shows the chain is reflected at x_0.

3.2. CTMC approximation of the Feynman–Kac semigroup and first passage probabilities

To approximate (2.4), we use $\mathbb{E}_x(f(Y_t) I(\zeta_Y > t))$, where ζ_Y is the lifetime of Y. This expectation is obtained in closed form in [40]; it is the approximate value function given the payoff

f and is calculated by

$$u_n(t, x) := \mathbb{E}_x \left(f(Y_t) I(\zeta_Y > t) \right) = \exp(\mathbb{G}_n t) f_n(x), \tag{3.6}$$

where $f_n = (f(x_0), \ldots, f(x_n))^T$ is an $(n+1)$-dimensional column vector, and $\exp(\mathbb{G}_n t) f_n(x)$ in (3.6) is the entry corresponding to x in the vector $\exp(\mathbb{G}_n t) f_n$.

One may also be interested in approximations of $P(t, x, l)$ and $p(t, x, y)$, where P is the distribution of X_t given that the process starts at x, and p is the corresponding density on the interior of the state space. We now denote the transition probability of the CTMC from x to y in time t by $P_n(t, x, y)$. It is given by

$$P_n(t, x, y) = \exp(\mathbb{G}_n t)(x, y), \qquad x, y \in \mathbb{S}_n^-,$$

which is the entry of the matrix $\exp(\mathbb{G}_n t)$ with its row corresponding to x and its column to y. In particular, $P_n(t, x, l)$ approximates $P(t, x, l)$. For $y \in \mathbb{S}_n^\circ$, define

$$p_n(t, x, y) := P_n(t, x, y)/\delta y, \qquad x \in \mathbb{S}_n^-.$$

Then we can approximate $p(t, x, y)$ by $p_n(t, x, y)$.

It is also of interest in practice to calculate the first passage probability $\mathbb{P}(\tau_z^X > t | X_0 = x)$ for $l \le x < z$, where τ_z^X is the hitting time of z of the sticky diffusion X. The paper [43] obtains a semi-analytical formula for this probability under the sticky OU model. We use CTMC approximation to calculate the probability for general sticky diffusions. Let Y be the CTMC that approximates X (set $k \equiv 0$ in $\mathbb{G}_n$). Then, for Y, using [40],

$$\mathbb{P}(\tau_z^Y > t | Y_0 = x) = \exp(\mathbb{H}_n t)\mathbf{1}(x),$$

where $\tau_z^Y = \inf\{t : Y_t > z\}$, $\mathbb{H}_n$ is the submatrix of $\mathbb{G}_n$ with entries corresponding to states smaller than z, and $\mathbf{1}$ is a vector of ones with dimension compatible with $\mathbb{H}_n$. In particular, setting $x = l$, we obtain an approximation of the first passage probability when the diffusion starts from the sticky boundary.

To implement the proposed method, we need to compute the matrix exponential, for which a variety of algorithms exist. In this paper we evaluate the performance of the three approaches listed below:

- The scaling and squaring algorithm of [24] is used widely in the literature on Markov chain approximation. It is known that this algorithm can handle all kinds of matrices, and it is numerically stable. It requires $O(n^3)$ operations to compute $\exp(\mathbb{G}_n t) f_n$.

- For the case when $\mathbb{G}_n$ is a tridiagonal matrix, [34] developed an algorithm based on the fast matrix eigendecomposition algorithm of [15], known as the MRRR algorithm. This algorithm takes only $O(n^2)$ operations to compute $\exp(\mathbb{G}_n t) f_n$.

- The third approach is to numerically solve the ODE system that the matrix exponential $\mathbb{F}$ satisfies, which is

$$d\mathbb{F}(t) = \mathbb{G}_n \mathbb{F}(t) dt, \qquad \mathbb{F}(0) = I_{n+1}.$$

  We propose to apply the extrapolation approach of [19], which has not previously been considered in the literature on CTMC approximation.

Our experiment in Section 5.1 shows that the third approach performs the best, and we recommend using it for computing $\exp(\mathbb{G}_n t)$, especially when t is large.

3.3. Eigenfunction expansions for the CTMC

We provide an eigenfunction expansion representation for $p_n(t, x, y)$, which will be utilized later to analyze the convergence rate of CTMC approximation. Let

$$M_n(x_0) = M(x_0) \exp\left(\frac{\alpha}{\sigma^2(x_0)} \delta^+ x_0\right), \tag{3.7}$$

$$\frac{1}{s_n(x_0)} = \rho M_n(x_0) = \exp\left(\frac{\alpha}{\sigma^2(x_0)} \delta^+ x_0\right),$$

where

$$\alpha = \begin{cases} \mu(x_0), & \text{Scheme 1,} \\ \rho, & \text{Scheme 2,} \end{cases} \tag{3.8}$$

and for $x = x_1, \ldots, x_n$,

$$m_n(x) = M_n(x_0) \beta \frac{2\rho}{-\mu(x_1)\delta^+ x_1 + \sigma^2(x_1)} \prod_{y=x_1}^{x^-} \frac{\mu(y)\delta^- y + \sigma^2(y)}{-\mu(y^+)\delta^+ y^+ + \sigma^2(y^+)}, \tag{3.9}$$

$$\frac{1}{s_n(x)} = \frac{1}{2} m_n(x)(\mu(x)\delta^- x + \sigma^2(x)),$$

where α is as in (3.8), β is as in (3.5), and the product term equals 1 if $x = x_1$. We also define $M_n(x) = m_n(x)\,\delta x$. As will be shown later, $m_n(x) \approx m(x)$ for $x \in \mathbb{S}_n^\circ$, and (3.7) shows that $M_n(x_0) \approx M(x_0)$. Furthermore, the last two terms in (3.9) are an approximation of $\int_{x_1}^{x} 2\mu(y)/\sigma^2(y)dy$, which appears in the definition of the scale density and speed density of the diffusion X. Hence, one can show that M_n, m_n, and s_n are candidates to approximate the speed measure, speed density, and scale density of the diffusion.

Recall the expression (3.1) for G_n, the generator of the CTMC. For $x \in \mathbb{S}_n^\circ$, we can rewrite it in the form

$$G_n g(x) = \frac{1}{m_n(x)} \frac{\delta^- x}{\delta x} \nabla^- \left(\frac{1}{s_n(x)} \nabla^+ g(x)\right) - k(x)g(x),$$

which is crucial for the convergence rate analysis.

Consider the eigenvalue problem of G_n:

$$\begin{aligned} G_n \varphi^n(x) &= -\lambda \varphi^n(x), & x &= x_0, \ldots, x_n, \\ \varphi^n(x_{n+1}) &= 0, \end{aligned} \tag{3.10}$$

where $\varphi^n(x)$ is defined on $\mathbb{S}_n$, i.e., it is a vector. Let $(\lambda_k^n, \varphi_k^n)$ be the kth eigenpair. The eigenvalue problem of the operator G_n in (3.10) is essentially the eigenvalue problem of the matrix $\mathbb{G}_n$, which is tridiagonal with negative diagonal elements and positive off-diagonal ones, and also diagonally dominant. Thus, it has $n + 1$ simple and real eigenvalues with $0 \le \lambda_1^n < \lambda_2^n < \ldots$ (see [34, Proposition 3.6]), and one expects $\lambda_k^n \approx \lambda_k$. For any two functions g_1, g_2 defined on $\mathbb{S}_n$, define their inner product $(g_1, g_2)_n := \sum_{x \in \mathbb{S}_n} g_1(x)g_2(x)M_n(x)$. Since eigenfunctions are only unique up to a constant, we normalize them to satisfy $(\varphi_j^n, \varphi_k^n)_n = \delta_{jk}$, so that $\varphi_k^n(x_i) \approx \varphi_k(x_i)$.

We have the following bilinear eigenfunction expansion representations:

$$P_n(t, x, y) = M_n(y) \sum_{k=1}^{n} \exp\left(-\lambda_k^n t\right) \varphi_k^n(x) \varphi_k^n(y), \qquad x \in \mathbb{S}_n^-, y \in \mathbb{S}_n^-, \tag{3.11}$$

$$p_n(t, x, y) = m_n(y) \sum_{k=1}^{n} \exp\left(-\lambda_k^n t\right) \varphi_k^n(x) \varphi_k^n(y), \qquad x \in \mathbb{S}_n^-, y \in \mathbb{S}_n^\circ. \tag{3.12}$$

3.4. CTMC approximation of 1D diffusions with a sticky interior point

We show how to construct a CTMC approximation for general diffusions with a sticky interior point $S^* \in \mathbb{S}^\circ$ (the boundary points are not sticky). To this end, one can generalize the steps in [26] and obtain the generator of this new diffusion as

$$\mathcal{G}f(x) = \begin{cases} \mu(x)f'(x) + \frac{1}{2}\sigma^2(x)f''(x) - k(x)f(x), & x \neq S^*, \\ \rho\left(f'(x+) - f'(x-)\right) - k(x)f(x), & x = S^*, \end{cases}$$

with domain

$$\mathcal{D} = \Big\{ f \in C^2\left(\mathbb{S} \setminus \{S^*\}\right) \cap C_b\left(\mathbb{S}\right) : \mathcal{G}f \in C_b\left(\mathbb{S}\right),$$

$$\rho\left(f'\left(S^*+\right) - f'\left(S^*-\right)\right) - k\left(S^*\right)f\left(S^*\right) = \lim_{x \to S^*} \mathcal{G}f(x) \Big\}.$$

By setting $S^* = l$, we recover the sticky lower boundary case as the left limit $f'(S^* -) = 0$. The CTMC that approximates this diffusion can be constructed as follows, and we call it Scheme 1. First, we put S^* on the grid, and the index for this state is denoted by j; i.e., $x_j = S^*$. Second, the transition rate matrix $\mathbb{G}_n$ is adjusted at x_j as follows:

$$\mathbb{G}_{n,j,j-1} = \frac{\rho}{\delta^- S^*}, \qquad \mathbb{G}_{n,j,j} = -\rho\frac{2\delta S^*}{\delta^- S^*\delta^+ S^*} - k\left(S^*\right), \qquad \mathbb{G}_{n,j,j+1} = \frac{\rho}{\delta^+ S^*}.$$

At the left boundary, the transition rate $\mathbb{G}_{n,0,1} = 0$ is set according to the behavior of the boundary point. See Remark 3 for the absorbing and reflecting cases.

We can also develop a scheme that achieves second-order convergence, which we call Scheme 2. Applying Taylor expansion yields

$$\nabla^+ f\left(S^*\right) = f'\left(S^*+\right) + \frac{1}{2}f''\left(S^*+\right)\delta^+ S^* + O(h_n^2), \tag{3.13}$$

$$\nabla^- f\left(S^*\right) = f'\left(S^*-\right) - \frac{1}{2}f''\left(S^*-\right)\delta^- S^* + O(h_n^2). \tag{3.14}$$

Since $f \in \mathcal{D}$, we also have

$$f''\left(S^*+\right) = \frac{\rho\left(f'\left(S^*+\right) - f'\left(S^*-\right)\right) - \mu\left(S^*+\right)f'\left(S^*+\right)}{\sigma^2\left(S^*+\right)/2},$$

$$f''\left(S^*-\right) = \frac{\rho\left(f'\left(S^*+\right) - f'\left(S^*-\right)\right) - \mu\left(S^*-\right)f'\left(S^*-\right)}{\sigma^2\left(S^*-\right)/2}.$$

Substituting these two equations in (3.13) and (3.14), we obtain

$$\nabla^+ f(S^*) = \left(1 + \frac{\rho - \mu(S^* +)}{\sigma^2(S^* +)}\delta^+ S^*\right)f'(S^* +) - \frac{\rho\delta^+ S^*}{\sigma^2(S^* +)}f'(S^* -) + O(h_n^2),$$

$$\nabla^- f(S^*) = \left(1 + \frac{\rho + \mu(S^* -)}{\sigma^2(S^* -)}\delta^- S^*\right)f'(S^* -) - \frac{\rho\delta^- S^*}{\sigma^2(S^* -)}f'(S^* +) + O(h_n^2).$$

Let

$$A = 1 + \frac{\rho - \mu(S^* +)}{\sigma^2(S^* +)} \delta^+ S^*,$$

$$B = \frac{\rho \delta^+ S^*}{\sigma^2(S^* +)},$$

$$C = 1 + \frac{\rho + \mu(S^* -)}{\sigma^2(S^* -)} \delta^- S^*,$$

$$D = \frac{\rho \delta^- S^*}{\sigma^2(S^* -)};$$

then

$$f'(S^* +) = \frac{C\nabla^+ f(S^*) + B\nabla^- f(S^*)}{AC - BD} + O(h_n^2),$$

$$f'(S^* -) = \frac{D\nabla^+ f(S^*) + A\nabla^- f(S^*)}{AC - BD} + O(h_n^2).$$

Therefore,

$$\rho\left(f'(S^* +) - f'(S^* -)\right) - k(S^*)f(S^*) = \frac{\rho(C - D)}{AC - BD}\nabla^+ f(S^*) + \frac{\rho(B - A)}{AC - BD}\nabla^- f(S^*)$$
$$- k(S^*)f(S^*) + O(h_n^2).$$

The corresponding elements of the generator matrix are then given by

$$\mathbb{G}_{n,j,j-1} = \frac{\rho(A - B)}{(AC - BD)\delta^- S^*}, \qquad \mathbb{G}_{n,j,j+1} = \frac{\rho(C - D)}{(AC - BD)\delta^+ S^*},$$

$$\mathbb{G}_{n,j,j} = -\mathbb{G}_{n,j,j-1} - \mathbb{G}_{n,j,j+1} - k(S^*).$$

Remark 4. Now suppose we have p sticky points, and the set of such points is $I_{S^*} = \{S_1^*, \ldots, S_p^*\}$, with ρ_i as the stickiness parameter at S_i^*. The generator of the process is given by

$$\mathcal{G}f(x) = \begin{cases} \mu(x)f'(x) + \frac{1}{2}\sigma^2(x)f''(x) - k(x)f(x), & x \notin I_{S^*}, \\ \rho_i\left(f'(x+) - f'(x-)\right) - k(x)f(x), & x = S_i^*, \quad i = 1, \ldots, p, \end{cases}$$

with domain

$$\mathcal{D} = \left\{ f \in C^2\left(\mathbb{S} \setminus I_{S^*}\right) \cap C_b\left(\mathbb{S}\right) : \mathcal{G}f \in C_b\left(\mathbb{S}\right),\right.$$

$$\left. \rho_i\left(f'\left(S_i^*+\right) - f'\left(S_i^*-\right)\right) - k\left(S_i^*\right)f\left(S_i^*\right) = \lim_{x \to S_i^*} \mathcal{G}f\left(S_i^*\right), \ i = 1, \ldots, p\right\}.$$

A sticky left or right boundary can be included in this framework by setting $f'\left(S_i^*-\right) = 0$ or $f'\left(S_i^*+\right) = 0$. One can then obtain the CTMC transition rates at each sticky point using finite differences in the same way as the single sticky point case.

4. Convergence rate analysis

In this section, we derive the convergence rates of two CTMC approximation schemes. The structure of our proof is similar to that in [55]. However, many details differ because of the change in the boundary behavior of the diffusion. In fact, some of the arguments in [55] do not hold for the sticky case.

We will analyze a sequence of grids satisfying the following assumption.

Assumption 3. *For a sequence of grids* $\{\mathbb{S}_n\}$ *with* $h_n \to 0$, *there exists a constant* $C > 0$ *independent of n such that for every grid* $\mathbb{S}_n$ *we have*

$$\frac{\max_{x \in \mathbb{S}_n^-} \delta^+ x}{\min_{x \in \mathbb{S}_n^-} \delta^+ x} \le C.$$

This assumption essentially says the maximum step size and the minimum step size should go to zero at comparable rates, which applies to all the types of grids used in practice.

Our convergence rate analysis hinges on the eigenfunction expansion representations in (2.9), (2.10), (3.11), and (3.12); it consists of the following main steps. First, we estimate the errors $M_n(x_0) - M(x_0)$, $m_n(x) - m(x)$, and $1/s_n(x) - 1/s(x)$ based on the expressions for these quantities. Second, we develop estimates for the errors of eigenvalues based on a min-max representation. Third, we obtain the errors of the eigenfunctions based on the errors of the eigenvalues. Fourth, we utilize the eigenfunction expansion representations and the error estimates for the eigenvalues and eigenfunctions to estimate $P_n(t, x, x_0) - P(t, x, x_0)$ and $p_n(t, x, y) - p(t, x, y)$. Finally, we obtain the estimates for $u_n(t, x) - u(t, x)$ using previous results and the representation (2.8). In the following, $\alpha = \mu(x_0)$ for Scheme 1 and $\alpha = \rho$ for Scheme 2.

Proposition 2. *Under Assumption 2, the approximation error for the speed measure and density satisfies*

$$M_n(x_0) - M(x_0) = M(x_0) \frac{\alpha}{\sigma^2(x_0)} \delta^+ x_0 + O(h_n^2), \tag{4.1}$$

$$m_n(x) - m(x) = m(x) \frac{\mu(x)}{\sigma^2(x)} \left(\delta^+ x - \delta^- x \right) + O(h_n^2), \qquad \forall x \in \mathbb{S}_n^\circ. \tag{4.2}$$

Furthermore, for $x \in \mathbb{S}_n^-$ *we have*

$$\frac{1}{s_n(x)} - \frac{1}{s(x)} = O(h_n). \tag{4.3}$$

Proposition 3. *Consider* $h_n \in (0, \delta)$, *where* δ *is sufficiently small. Then there exists a constant* $C > 0$ *such that for any* $k \le h_n^{-1/4}$,

$$\left| \lambda_k^n - \lambda_k \right| \le Ck^4 h_n^\gamma, \tag{4.4}$$

where C is independent of k and n, $\gamma = 1$ *for Scheme 1, and* $\gamma = 2$ *for Scheme 2.*

Proposition 4. *Suppose Assumptions 2 and 3 hold, and consider* $h_n \in (0, \delta)$, *where* δ *is sufficiently small. Then there exists a constant* $C > 0$ *independent of k and n such that for* $1 \le k \le h_n^{-1/5}$ *the following holds:*

$$\left\| \varphi_k^n - \varphi_k \right\|_{n,\infty} \le Ck^4 h_n^\gamma. \tag{4.5}$$

Here, $\gamma = 1$ *for Scheme 1 and* $\gamma = 2$ *for Scheme 2.*

Theorem 3. *Suppose Assumptions 2 and 3 hold, and consider $h_n \in (0, \delta)$, where δ is sufficiently small. For any $t > 0$, $x \in \mathbb{S}_n^-$, and $y \in \mathbb{S}_n^\circ$, we have*

$$p_n(t, x, y) - p(t, x, y) = p(t, x, y)\left(\frac{\mu(y)}{\sigma^2(y)}\left(\delta^+ y - \delta^- y\right)\right) + C_t h_n^\gamma,$$

$$P_n(t, x, x_0) - P(t, x, x_0) = P(t, x, x_0)\left(\frac{\alpha}{\sigma^2(x_0)}\delta^+ x_0\right) + C_t h_n^\gamma,$$

where $C_t > 0$ depends only on t and is independent of n, x_0, x, and y, and where $\gamma = 1$ for Scheme 1 and $\gamma = 2$ for Scheme 2.

The value function under the CTMC model is given by

$$u_n(t, x) = \sum_{y \in \mathbb{S}_n^-} P_n(t, x, y) f(y) = P_n(t, x, x_0) f(x_0) + \sum_{y \in \mathbb{S}_n^\circ} p_n(t, x, y) f(y) \delta y. \qquad (4.6)$$

Using (2.8) and (4.6) together with the estimates in Theorem 3, we can estimate the difference $u_n(t, x) - u(t, x)$, which also depends on the smoothness of the payoff function f. In the following discussions, we simply assume that there exists a point $\xi \in (l, r)$ at which f may not be smooth. Specifically, f is C^2 on $(l, \xi) \cup (\xi, r)$, and ξ is a non-smooth point with either $f(\xi-) \neq f(\xi+)$ or $f(\xi-) = f(\xi+)$ but $f'(\xi-) \neq f'(\xi+)$. These types of payoffs are common in financial applications. The result can be easily extended to handle multiple non-smooth points.

Theorem 4. *Under Assumptions 2 and 3, there exist constants C_t, $D_t > 0$, independent of n, such that*

$$\|u_n(t, \cdot) - u(t, \cdot)\|_{n,\infty} \leq \sup_{x \in [l,r)} p(t, x, \xi) |f(\xi-) - f(\xi+)| \left|\frac{\xi^- + \xi^+}{2} - \xi\right| + C_t h_n^\gamma,$$

$$|u_n(t, x) - u(t, x)| \geq p(t, x, \xi) |f(\xi-) - f(\xi+)| \left|\frac{\xi^- + \xi^+}{2} - \xi\right| - D_t h_n^\gamma.$$

Here, D_t is also independent of x, $\gamma = 1$ for Scheme 1, and $\gamma = 2$ for Scheme 2.

This theorem shows that for Scheme 1, convergence is only first-order, regardless of how non-smooth f is at ξ. For Scheme 2, discontinuity in the first-order derivative does not change the convergence order; however, discontinuity in the payoff undermines the order. A simple grid design that would restore second-order convergence for Scheme 2 is to place ξ halfway between two grid points. This midpoint rule was proposed and validated in [55] for diffusions with two killing boundaries.

The convergence rate for the first passage probability $\mathbb{P}(\tau_z^X > t | X_0 = x)$ can be analyzed in essentially the same way. One can treat z as a killing boundary for the diffusion and assume that z is on the CTMC grid. The estimates in Theorem 4 apply with the payoff f identically 1, so convergence is first-order for Scheme 1 and second-order for Scheme 2. It is important to place the passage level z on the grid as explained in [55, Section 4.5]; otherwise convergence becomes first-order even for Scheme 2.

Remark 5. For the sticky interior point case, we can also prove that Scheme 1 is first-order and Scheme 2 is second-order. There are three main steps to show convergence of u_n to u.

TABLE 1: Model parameters for the sticky OU process.

Model	κ	θ	σ	ρ	x
1	0.4500	0.1000	0.0500	4.0×10^{-3}	0.0100
2	0.7500	0.0500	0.0150	1.0×10^{-6}	0.0010
3	0.2210	0.2000	0.0170	5.8×10^{-5}	0.0000

First, we can show that $(\mathbb{G}_n - \mathcal{G})g = O(h_n^\gamma)$ for some function g, where γ equals 1 for Scheme 1 and 2 for Scheme 2. Second, we need to define m_n, M_n, and s_n appropriately to show that they converge to the speed density, speed measure, and scale density of the diffusion. The main results of Propositions 2–4 still hold. Finally, all other results can be obtained in an analogous way following the steps in the proof for the sticky lower boundary case.

5. Two financial applications of sticky diffusions

We demonstrate the usefulness of our method by studying two distinct types of processes: a sticky OU process and a geometric Brownian motion with switching drift and volatility coefficients.

5.1. Numerical results for the sticky OU short-rate model

The sticky OU process is given by the following SDE:

$$dX_t = (\kappa (\theta - X_t) I (X_t > 0) + \rho I (X_t = 0)) dt + \sigma I (X_t > 0) dB_t,$$

where $l = 0$ is the left boundary. This process is used in [42] (and also in [43]) to model short rates, which are instantaneous interest rates. The advantages of using this model over standard short-rate models are explained in [42]. In particular, this model is able to produce various shapes of yield curves observed in the market, including the S-shaped yield curve in a low-interest environment seen after the 2008 financial crisis. To illustrate this point, we consider three different sets of values for the parameters of a sticky OU process, which are listed in Table 1. These sets are able to produce three different shapes of yield curves: upward-sloping (Model 1), inverted (Model 2), and S-shaped (Model 3). In general, the magnitude of the stickiness parameter plays an important role in controlling the shape of the curve. Calibration shows that the implied stickiness parameter from real market data is on similar scales with the values in the table (see [42]).

Throughout this section, we consider pricing zero-coupon bonds with unit payoff, i.e. $u(t, x) = \mathbb{E}_x(\exp(-\int_0^t X_u du))$ with $k(x) = x$. The paper [43] obtained an eigenfunction expansion formula for the bond price under the sticky OU model. We use the method of [43] to obtain benchmarks for our method. Table 2 shows the absolute difference between the results of the CTMC method with 20,000 grid points and the eigenfunction expansion method using 50 to 100 terms in the expansion.

It can be seen that these methods yield consistent results for all maturities shown in the table. The eigenfunction expansion method can be slow for small maturities (e.g., 1 or 3 months). This is because the nth term in the expansion involves $e^{-\lambda_n t}$ (see [43, Proposition 4.2]), where λ_n is the nth eigenvalue and t is the time to maturity. This exponential term decays slowly for small t, so more terms in the expansion are required to achieve good accuracy.

TABLE 2: Differences in prices for the CTMC method and the eigenfunction expansion method of [42, Section 6].

Maturity	6M	1Y	2Y	3Y	10Y	20Y	30Y
Model 1	7.98E-10	2.90E-09	9.88E-09	9.24E-09	8.13E-08	1.28E-07	1.40E-07
Model 2	9.74E-08	1.48E-07	4.71E-07	8.71E-07	3.50E-06	6.04E-06	7.65E-06
Model 3	1.14E-05	9.86E-06	7.34E-06	5.43E-06	2.03E-06	9.41E-06	1.48E-05

5.2. Convergence rates

We localize the state space $[0, \infty)$ to $[0, 1]$. Simple calculations show that for the OU process with parameter values in Table 1, the probability of breaching this upper boundary is extremely small for all maturities under consideration, and hence the localization error is negligible. We then discretize $[0, 1]$ with $n = 100, 200, 400, 800, 1600$ points using a uniform grid and apply the squaring and scaling algorithm to calculate the matrix exponential. The convergence rate is detected numerically. Figure 1 plots the results for three models with two maturities. It is clear that for Models 1 and 3, Scheme 2 converges at second order while Scheme 1 only attains first order; this can be seen by checking the slope of the convergence line against that of the small triangle in the lower left corner of each plot. This validates our theoretical estimates in Theorem 4. For Model 2, the convergence orders of Scheme 1 and Scheme 2 are both around two. This may at first seem unexpected, but the value of ρ is very small in this model (much smaller than in the other two models), which makes $\mathbb{G}_{n,0,1}$ roughly zero under both schemes. So the two schemes perform similarly.

We can further observe that in Models 2 and 3, Scheme 1 is more accurate than Scheme 2 for small n. The reason is that $\mathbb{G}_{n,0,1}$ is always positive in Scheme 1, whereas it can become negative in Scheme 2. In the latter case, the matrix $\mathbb{G}_n$ is not a proper transition rate matrix, which leads to larger errors near the boundary. Finally, for all models it is observed that the absolute error is greater when the maturity is longer.

A practical question is which scheme should be used. The choice depends on the parameter values. When ρ is extremely small (like the value of ρ in Model 2), we recommend Scheme 1 for the reasons mentioned above. For moderate and big values of ρ, one can always implement Scheme 2 if highly accurate results are needed.

5.3. Some comparisons

The calculation of the value function under the CTMC model is based on the calculation of the matrix exponential. In this section, we compare three ways of computing the matrix exponential in our problem (the three ways listed in Section 3.2), and we also compare the CTMC approximation algorithm with a standard finite difference scheme.

We now briefly describe the extrapolation approach of [19] for numerically solving the ODE system satisfied by the matrix exponential. This approach uses a basic step size H, where $H = 0.5$ if the maturity T is greater than 0.5 and $H = T$ otherwise, to divide the interval $[0,T]$ into smaller time periods. For each basic interval, $M_i = 1, \ldots, s$ time steps are used to evolve the differential equation according to the implicit scheme to calculate the matrix exponential, where $s \geq 1$ denotes the extrapolation stage number. Let the approximation of the solution after one basic step be denoted by $A_{i,1} = u_n(H, x; M_i)$ where M_i time points are used for the interval
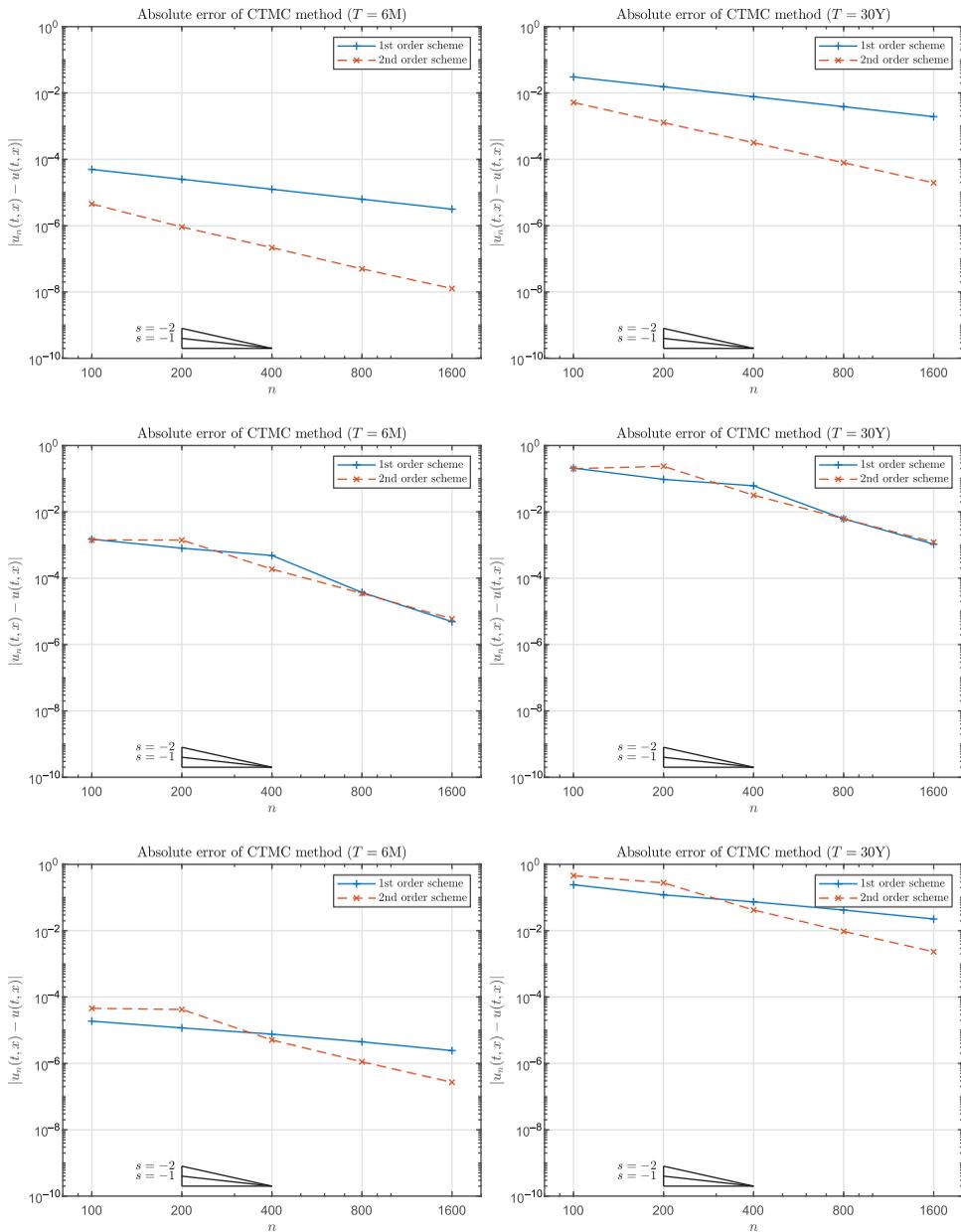
FIGURE 1: Absolute error vs. *n* on log-log scale for Models 1–3 (from top to bottom) with six-month and 30-year maturities.

[0,*H*]. An extrapolation tableau is constructed by the equation

$$A_{i,j} = A_{i-1,j-1} + \frac{A_{i,j-1} - A_{i-1,j-1}}{\frac{M_i}{M_{i-j+1}} - 1},$$

for $i = 2, \ldots, s$ and $j = 2, \ldots, i$. We then use the value $A_{s,s}$ after s extrapolation steps as the starting point of the approximation over the time interval [*H*, 2*H*]. This calculation of

approximations after basic steps is repeated until one obtains an approximation of $u_n(T, x)$ after M basic steps, where $T = MH$. Finally, the value of $A_{s,s}$ after M steps is the approximation of the zero-coupon bond price with maturity T at time 0.

For the finite difference scheme, which discretizes both time and space in the PDE satisfied by the value function of the sticky diffusion, we use Crank–Nicolson time-stepping, which is a standard choice in the literature for numerical solutions of PDEs. It is also considered in [42]. We use equal time steps with 5 steps in a month. This allows for an adequate number of time steps even for longer maturities.

The MRRR algorithm, the extrapolation approach, and the finite difference method are implemented in C++, whereas the scaling and squaring method is already implemented in Matlab so we directly call it in Matlab. Although a Matlab implementation may generally be less efficient than an equivalent C++ implementation, it does not affect the conclusion that the scaling and squaring method is typically the slowest for obtaining similar levels of accuracy, as it involves the highest amount of computational complexity.

The results are obtained using a workstation running CentOS 7 with 3.2 GHz CPUs (32 cores) and memory of 256 GB. We did not make use of parallelization or other methods to speed up computations. The workstation was used because a larger amount of memory is needed to store the matrix exponential when calculating the benchmark prices with 20,000 grid points. All numerical calculations were run 10 times to obtain the average running time. Figure 2 displays a comparison of the three models for bonds with one-year and 30-year maturities.

The comparison clearly favors the extrapolation method, which defeats the other three methods in all cases, and its leading edge becomes greater as the bond's maturity increases. It should be noted that the eigendecomposition method based on the MRRR algorithm does not always work. For Model 2, it cannot be applied when n is too large, and for Model 3, it fails for $n = 100$ because of overflow/underflow errors in calculating a similar symmetric tridiagonal matrix required by the algorithm.

5.4. Simulation

We also consider how to perform simulations for sticky diffusions. Our CTMC approximation method offers a natural alternative to the standard Euler scheme. The simulation of sample paths from a CTMC is straightforward, and unlike the Euler scheme, it does not require time-discretization. We use 500 grid points for the CTMC Y constructed by Scheme 2, start with $Y_0 = x$, and then draw an exponentially distributed random variable with intensity $|\mathbb{G}_{n,x,x}|$ to determine the amount of time spent in the initial state. After determining the time point when the Markov chain is transitioning, we use the transition rates $\mathbb{G}_{n,x,x^-}$, $\mathbb{G}_{n,x,x^+}$, and $k(x)$ to sample the new state. These steps are repeated until maturity is reached. Using the definition of the order of weak convergence given in [21] and [29] together with Theorem 4, we find that the weak convergence order of the CTMC simulation scheme using the transition rate matrix under Scheme 2 is two (it is one if Scheme 1 is used).

The Euler scheme is implemented in the following way. Time is discretized using 50 time steps per month. The process starts with $X_0 = x$, and subsequent values of the process are computed using the discretization of the SDE (2.3). In particular, for $t = 0, \Delta t, \ldots, T - \Delta t$,

$$Z_{t+\Delta t} = \begin{cases} X_t + \mu(X_t)\,\Delta t + \sigma(X_t)\,\sqrt{\Delta t}\xi_{t+\Delta t} & \text{if } X_t > 0, \\ \rho\,\Delta t & \text{if } X_t = 0, \end{cases}$$

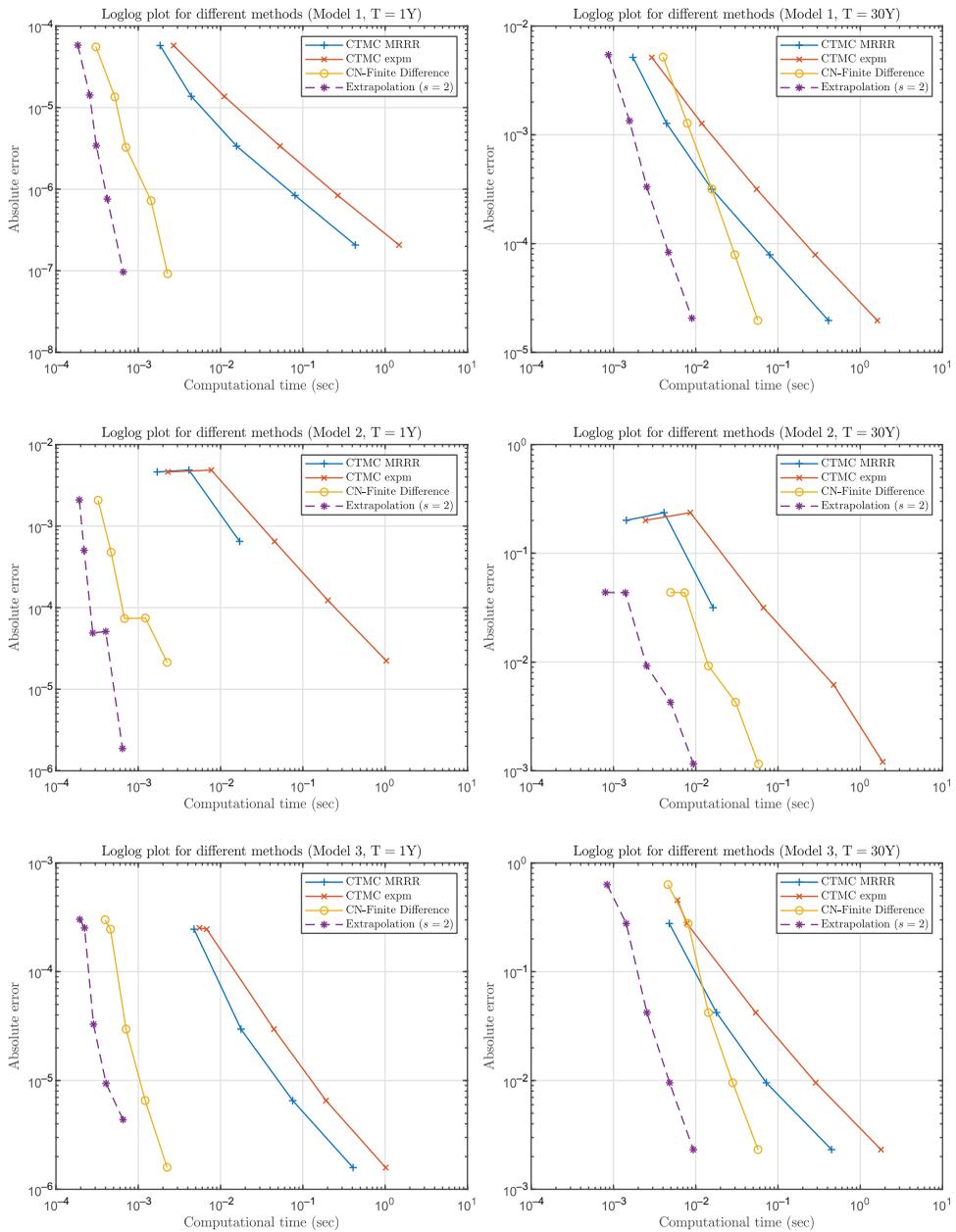$$e_{t+\Delta t} \sim \text{Exp}(1),$$

FIGURE 2: Comparison of four methods. 'CTMC expm' stands for using the scaling and squaring algorithm for computing the matrix exponential in the CTMC method. In the extrapolation approach, extrapolation is only applied once (i.e., $s = 2$).
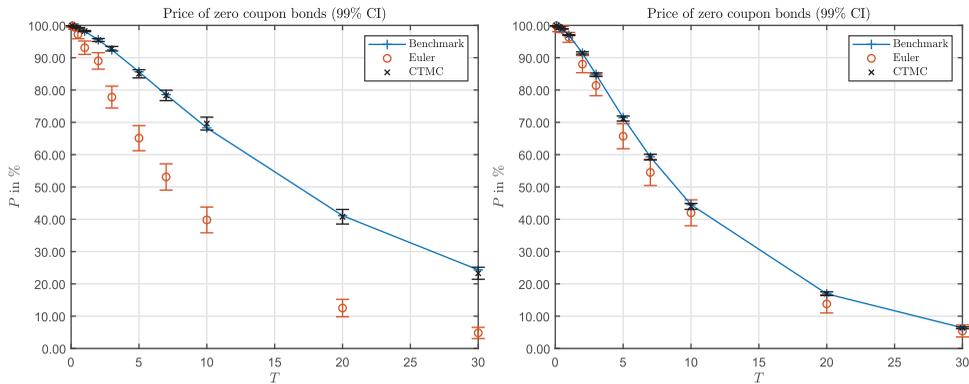
FIGURE 3: Monte Carlo simulation results for zero-coupon bond pricing. The blue line indicates the benchmark prices. The left panel shows the results for Model 1 with $\rho = 4.0 \times 10^{-3}$. In the right panel, the results are obtained by setting $\rho = 0.1$ with all other parameters remaining fixed.

where $\xi_{t+\Delta t}$ is standard normally distributed and $e_{t+\Delta t}$ is exponentially distributed with rate 1. The new value $Z_{t+\Delta t}$ is accepted as given by

$$
X_{t+\Delta t} = \begin{cases} Z_{t+\Delta t} & \text{if } Z_{t+\Delta t} > 0, \ e_{t+\Delta t} > k(X_t) \Delta t, \\ 0 & \text{if } Z_{t+\Delta t} \leq 0, \ e_{t+\Delta t} > k(X_t) \Delta t, \\ \partial & \text{if } e_{t+\Delta t} \leq k(X_t) \Delta t, \end{cases}
$$

where ∂ is the cemetery state and $f(\partial) = 0$.

Figure 3 shows the Monte Carlo simulation results when sample paths are simulated by a CTMC and the Euler scheme. In both cases, 1000 samples paths are simulated and the price estimator together with the 99% confidence intervals are displayed. The Euler scheme clearly fails when ρ is small, i.e., when the process is very sticky. However, it becomes acceptable when ρ is big enough. In contrast, the CTMC simulation scheme works well regardless of the degree of stickiness.

We provide some intuition about why the Euler scheme flops in very sticky cases. Note that this method only simulates a discrete-time process. If at some time point on the grid, say $i\Delta t$, the process is at zero, it moves to $\rho \Delta t$ at $(i + 1)\Delta t$. If Δt is small enough, the interpolated path of the Euler scheme should resemble the path of the continuous-time process to which the Euler scheme converges in the limit. Thus, it is intuitively clear that the limiting continuous-time process is instantaneously reflected at zero and hence not sticky there. When the original diffusion is only mildly sticky, it is not very different from the reflected case, so the Euler scheme produces acceptable results. However, if the original diffusion is very sticky, the difference from the reflected case is large and the results of the Euler scheme become useless. Figure 4 shows one path simulated from the CTMC scheme and the other from the Euler scheme. The CTMC simulation scheme does not discretize time, so it can generate the phenomenon that the process sticks to zero, whereas the Euler scheme cannot.

5.5. Geometric Brownian motion with a sticky interior point

We consider the model proposed in [26], where the asset price follows $dX_t = \mu(X_t)dt + \sigma(X_t)dB_t$ with $\mu(x) = (\mu_1 I(x < S^*) + \mu_2 I(x \geq S^*))x$ and $\sigma(x) = (\sigma_1 I(x < S^*) + \sigma_2 I(x \geq S^*))x$. We set $\mu_1 = 0.1$, $\mu_2 = 0.2$, $\sigma_1 = 0.3$, and $\sigma_2 = 0.4$, and the process starts at $X_0 = 100$. We
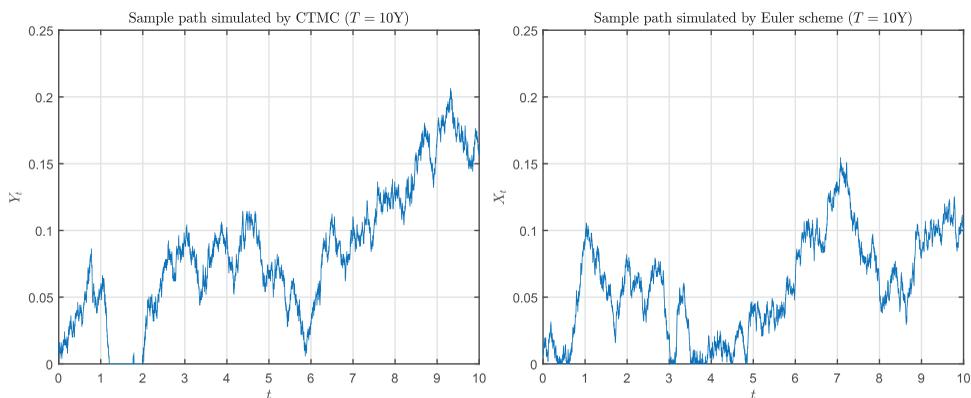
FIGURE 4: Sample paths over 10 years generated by the CTMC and Euler scheme. The sample path for the Euler scheme was simulated using $\Delta t = 1/600$, i.e., with 50 time steps per month.
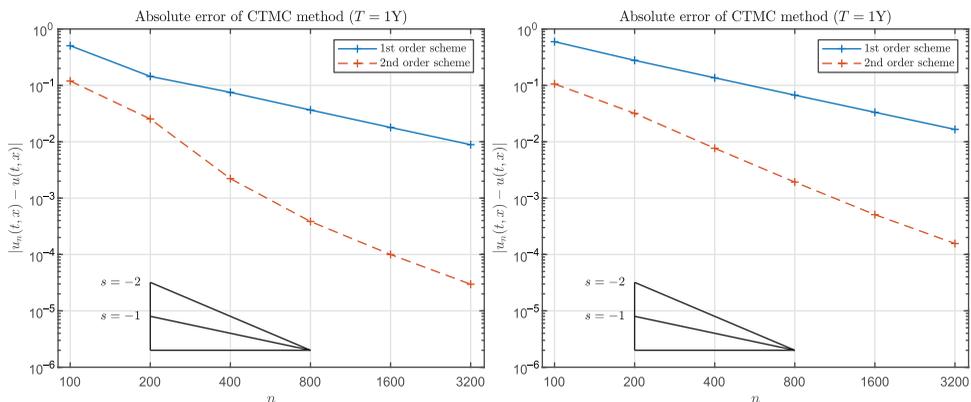

FIGURE 5: Absolute error vs. n on log-log scale for call option prices with one-year maturity obtained with the CTMC method: $S^* = 110$ (left) and $S^* = 90$ (right). The geometric Brownian motion is localized to [0,1000], and the scaling and squaring algorithm is used to compute matrix exponentials.

consider two cases, $S^* = 110$ and $S^* = 90$, and calculate the price of a European call option with strike price $\xi = 100$. The risk-free rate is 5%, and time to maturity equals one year. The stickiness at S^* is given by $\rho = 1/(2 \times 0.02) = 25$. To obtain benchmark prices, we apply the method in [26] to numerically invert the Laplace transform of the option price which was derived by the authors of [26]. However, for more general diffusion models, explicit formulas for the Laplace transform may not be available.

To implement the CTMC approximation method, we use the grid design in [55] which places the strike price K midway between two adjacent grid points. This would make convergence smooth for call options. In our design, we also place the sticky point S^* on the grid. Figure 5 shows convergence results for the two cases, from which the convergence orders for Scheme 1 and Scheme 2 are confirmed to be one and two. It should be noted that the initial price X_0 at which the option is priced is not on the grid, as $X_0 = K$. In this case, we used cubic splines to interpolate the prices on the neighboring grid points to obtain the price at X_0. This does not reduce the convergence order of CTMC approximation, as a cubic spline interpolation has higher convergence order.

6. Conclusion

This paper develops a CTMC approximation of one-dimensional diffusions with sticky boundary or interior points. A direct finite difference approximation of the generator of the diffusion at the sticky point leads to a first scheme, which only converges at first order. Matching the first and second moments of the infinitesimal changes at the sticky point, we obtain a second scheme, which is second-order. Under the CTMC model, calculations of the action of the Feynman–Kac operator and first passage probabilities can be obtained in closed form using matrix exponentials. Our method has several nice features. First, it is applicable to sticky diffusions with general drift, volatility, and killing rate. Second, it is computationally efficient. We show that when the extrapolation method of [19] is used to solve the ODE system for the matrix exponential, our method outperforms a standard finite difference scheme that is often used for solving diffusion PDEs. Third, the CTMC can be used to simulate the sticky diffusion, and it produces good results, whereas the Euler scheme completely fails when the diffusion is very sticky.

It is possible to define multidimensional sticky diffusions (see [22] and [25, Section IV.7]). A CTMC approximation can be constructed for these processes, but it suffers from the curse of dimensionality. Furthermore, analyzing its convergence rate based on spectral representations will be more difficult, as certain properties, like the simplicity of the spectrum or the asymptotics of the eigenvalues, may not be available in higher dimensions. For multidimensional sticky diffusions, it is important to develop efficient simulation schemes. As CTMC approximation can be used to produce sticky behavior in the interior or at the boundary, we expect that combining CTMC approximation with traditional simulation schemes will lead to computationally efficient algorithms; we plan to work in this direction in our future research.

Appendix A. Proofs

This appendix contains the proofs of major results of the paper. Additional proofs can be found in the online supplement.

Proof of Proposition 1: Application of the Liouville transform $h_1(x) = \int_l^x 1/\sigma(z)\, dz$ and a linear transformation $h_2(y) = -2y/B + 1$, where $B = h_1(r)$, changes the problem into

$$-\frac{2}{B^2}\psi''(z) + q(z)\,\psi(z) = \lambda\psi(z), \qquad z \in (-1, 1),$$

$$\psi(-1) = 0, \qquad -\frac{2\rho}{Bh_3(0)}\psi'(1) = \left(k(l) - \frac{h_4(0)}{\rho} - \lambda\right)\psi(1),$$

where

$$\psi(z) = \frac{\tilde{\varphi}\left(h_1^{-1}\left(h_2^{-1}(z)\right)\right)}{\sqrt{\sigma\left(h_1^{-1}\left(h_2^{-1}(z)\right)\right) s\left(h_1^{-1}\left(h_2^{-1}(z)\right)\right)}}, \tag{A.1}$$

$$q(z) = U\left(h_1^{-1}\left(h_2^{-1}(z)\right)\right) \qquad \text{and } U \text{ is the potential function,}$$

$$h_3(y) = \frac{\left(h_1^{-1}(y)\right)'}{\sqrt{\sigma\left(h_1^{-1}(y)\right)}}, \qquad h_4(y) = \frac{\left(\sigma\left(h_1^{-1}(y)\right) s\left(h_1^{-1}(y)\right)\right)'}{2\sigma\left(h_1^{-1}(y)\right) s\left(h_1^{-1}(y)\right)},$$

and $\tilde{\varphi}$ and ψ are the eigenfunctions of the original and the transformed problem. It should be noted that $\tilde{\varphi}$ denotes the eigenfunction and φ the normalized eigenfunction of the original problem. The potential function is defined in [36, Equation (3.31)].

This setting resembles the setting in [1], with $a_1 = a_2 = 2/B^2$ and $\gamma_i = \delta_i = 1$ for $i = 1, 2$, which allows the transmission condition to disappear, and the solution and its derivatives are continuous in $[-1, 1]$. Further following [1], let $\alpha_1 = 1$ and $\alpha_2 = 0$, and fix $\beta_1' = -1$, $\beta_2' = 0$, and $\beta_2 \neq 0$. It should be noted that because $\beta_2' = 0$, it is unimportant what value β_1' takes, and normalization to 1 is a simplification of notation.

The results in [1, Section 4] then show that the kth eigenvalue of the problem in Liouville normal form satisfies the asymptotic representation

$$\lambda_k = \frac{a_1^2 k^2 \pi^2}{4} - a_1 \beta_2 + \frac{1}{2a_1} \int_{-1}^{1} q(z)\, dz + O\left(\frac{1}{k}\right), \tag{A.2}$$

and so $C_1 k^2 \leq \lambda_k \leq C_2 k^2$ for constants $C_1, C_2 > 0$ independent of k. Using [1, Theorem 3.1] with trigonometric calculations, we have that for any $x \in [-1, 1]$,

$$\psi_k(x) = -\frac{a_1}{\sqrt{\lambda_k}} \sin \frac{\sqrt{\lambda_k}\,(x+1)}{a_1} + \frac{1}{a_1 \sqrt{\lambda_k}} \int_{-1}^{x} \sin \frac{\sqrt{\lambda_k}\,(x-z)}{a_1} q(z)\, \psi_k(z)\, dz. \tag{A.3}$$

Then

$$|\psi_k(x)| \leq \frac{a_1}{\sqrt{\lambda_k}} + \frac{1}{a_1 \sqrt{\lambda_k}} \int_{-1}^{x} |q(z)|\, |\psi_k(z)|\, dz \leq \frac{C_3}{\sqrt{\lambda_k}} + \frac{C_3}{\sqrt{\lambda_k}} \int_{-1}^{x} |q(z)|\, |\psi_k(z)|\, dz$$

for some constant $C_3 > 0$. The Gronwall inequality shows that

$$|\psi_k(x)| \leq \frac{C_3}{\sqrt{\lambda_k}} \exp\left(\int_0^B \frac{C_3\, |q(z)|}{\sqrt{\lambda_k}} dz\right) \leq \frac{C_4}{k}$$

for a constant $C_4 > 0$ independent of k and x, using the asymptotic representation of λ_k in (A.2).

Furthermore, for the first derivative we have

$$|\psi_k'(x)| \leq \left| -\cos \frac{\sqrt{\lambda_k}\,(x+1)}{a_1} + \frac{1}{a_1^2} \int_{-1}^{x} \cos \frac{\sqrt{\lambda_k}\,(x-z)}{a_1} q(z)\, \psi_k(z)\, dz \right|$$

$$\leq 1 + \frac{C_5}{k} \int_{-1}^{x} |q(z)|\, dz \leq C_6,$$

where $C_5, C_6 > 0$ are constants independent of k and x.

Similar bounds can be established for further derivatives, i.e. for $j = 2, 3, 4$, by differentiation of (A.3). Hence, one derives that $|\psi_k^{(j)}(x)| \leq C_7 k^{j-1}$. Finally, by [41, Theorem 4.2] it follows that

$$\|\psi_k\|_2 = \frac{C_8}{\pi k} + O(1/k^2) \geq C_9/k.$$

The normalized eigenfunctions then have the following asymptotic representation:

$$\frac{\psi_k(x)}{\|\psi_k\|_2} \leq \frac{C_2/k}{C_9/k} \leq C_{10}.$$

Using the relationship between $\tilde{\varphi}$ and ψ in (A.1) and the fact that σ and s are bounded on $\mathbb{S}$, one derives $\tilde{\varphi}_k(x) = O(1/k)$ and $\|\tilde{\varphi}_k\|_2 \geq C_{11}/k$. This implies that for all $x \in \mathbb{S}$, $\varphi_k(x) = \tilde{\varphi}_k(x)/\|\tilde{\varphi}_k\| = O(1)$. Using similar arguments, one can prove $\varphi_k^{(j)}(x) = O(k^j)$ for all $x \in \mathbb{S}$, $j = 1, \ldots, 4$. $\qquad\square$

Proof of Proposition 2: We will prove the claim first for x_0, then for x_1, and finally for all $x = x_2, \ldots, x_n$. First, note that

$$M_n(x_0) - M(x_0) = M(x_0) \exp\left(\frac{\alpha}{\sigma^2(x_0)}\delta^+ x_0\right) - M(x_0)$$

$$= M(x_0)\frac{\alpha}{\sigma^2(x_0)}\delta^+ x_0 + O(h_n^2).$$

In a second step, applying the logarithm to (3.9) for $x = x_1$ yields

$$\log m_n(x_1) = \log M_n(x_0) + \log \beta + \log \rho + \frac{\mu(x_1)}{\sigma^2(x_1)}\delta^+ x_1 + O(h_n^2)$$

$$+ \log \frac{2}{\sigma^2(x_1)} + \left(\frac{\mu(x_0)}{\sigma^2(x_0)} + \frac{\mu(x_1)}{\sigma^2(x_1)}\right)\delta^+ x_0 - \left(\frac{\mu(x_0)}{\sigma^2(x_0)} + \frac{\mu(x_1)}{\sigma^2(x_1)}\right)\delta^+ x_0$$

$$= \log M(x_0) + \frac{\alpha}{\sigma^2(x_0)}\delta^+ x_0 + \log \beta - \log M(x_0) + O(h_n^2)$$

$$+ \log m(x_1) + \frac{\mu(x_1)}{\sigma^2(x_1)}\left(\delta^+ x_1 - \delta^- x_1\right) - \frac{\mu(x_0)}{\sigma^2(x_0)}\delta^+ x_0$$

$$= \log m(x_1) + \frac{\mu(x_1)}{\sigma^2(x_1)}\left(\delta^+ x_1 - \delta^- x_1\right) + O(h_n^2),$$

where we used that

$$\log m(x_1) = \log \frac{2}{\sigma^2(x_1)} + \int_{x_0}^{x_1} \frac{2\mu(y)}{\sigma^2(y)}dy$$

$$= \log \frac{2}{\sigma^2(x_1)} + \left(\frac{\mu(x_0)}{\sigma^2(x_0)} + \frac{\mu(x_1)}{\sigma^2(x_1)}\right)\delta^+ x_0 + O(h_n^2)$$

and

$$\frac{\alpha}{\sigma^2(x_0)}\delta^+ x_0 + \log \beta - \frac{\mu(x_0)}{\sigma^2(x_0)}\delta^+ x_0$$

$$= \begin{cases} 0 & \text{for Scheme 1,} \\ \frac{\rho}{\sigma^2(x_0)}\delta^+ x_0 - \frac{\rho - \mu(x_0)}{\sigma^2(x_0)}\delta^+ x_0 - \frac{\mu(x_0)}{\sigma^2(x_0)}\delta^+ x_0 + O(h_n^2) & \text{for Scheme 2.} \end{cases} \quad (A.4)$$

Thus these terms equal 0 for Scheme 1 and are $O(h_n^2)$ for Scheme 2.

Now let $x \in \{x_2, \ldots, x_n\}$; then applying the logarithm to (3.9) and using the Taylor expansion for the logarithm yields

$$\log m_n(x) = \log M_n(x_0) + \log \beta + \log \rho + \frac{\mu(x)}{\sigma^2(x)}\left(\delta^+ x - \delta^- x\right) + \frac{\mu(x_1)}{\sigma^2(x_1)}\delta^- x_1$$

$$+ \log \frac{2}{\sigma^2(x)} + \sum_{y=x_1}^{x^-}\left(\frac{\mu(y)}{\sigma^2(y)} + \frac{\mu(y^+)}{\sigma^2(y^+)}\right)\delta y + \left(\frac{\mu(x_0)}{\sigma^2(x_0)} + \frac{\mu(x_1)}{\sigma^2(x_1)}\right)\delta^+ x_0$$

$$-\left(\frac{\mu\left(x_0\right)}{\sigma^2\left(x_0\right)} + \frac{\mu\left(x_1\right)}{\sigma^2\left(x_1\right)}\right)\delta^+x_0 + O(h_n^2)$$

$$= \log M_n\left(x_0\right) + \log\beta + \log\rho + \frac{\mu(x)}{\sigma^2(x)}\left(\delta^+x - \delta^-x\right)$$

$$+ \log m(x) - \frac{\mu\left(x_0\right)}{\sigma^2\left(x_0\right)}\delta^+x_0 + O(h_n^2),$$

where we used

$$\sum_{y=x_1}^{x^-}\left(\frac{\mu\left(y\right)}{\sigma^2\left(y\right)} + \frac{\mu\left(y^+\right)}{\sigma^2\left(y^+\right)}\right)\delta y + \left(\frac{\mu\left(x_0\right)}{\sigma^2\left(x_0\right)} + \frac{\mu\left(x_1\right)}{\sigma^2\left(x_1\right)}\right)\delta^+x_0 = \int_{x_0}^x\frac{2\mu\left(y\right)}{\sigma^2\left(y\right)}dy + O(h_n^2)$$

and

$$\log m(x) = \log\frac{2}{\sigma^2(x)} + \int_{x_0}^x\frac{2\mu\left(y\right)}{\sigma^2\left(y\right)}dy.$$

Furthermore, using $M\left(x_0\right) = \frac{1}{\rho}$ and (3.7) yields

$$\log m_n(x) = \frac{\alpha}{\sigma^2\left(x_0\right)}\delta^+x_0 + \log\beta - \frac{\mu\left(x_0\right)}{\sigma^2\left(x_0\right)}\delta^+x_0 + \frac{\mu(x)}{\sigma^2(x)}\left(\delta^+x - \delta^-x\right) + \log m(x) + O(h_n^2).$$

Therefore, by using (A.4), we obtain from the previous result that

$$m_n(x) - m(x) = m(x)\left(\frac{\mu(x)}{\sigma^2(x)}\left(\delta^+x - \delta^-x\right)\right) + O(h_n^2).$$

Hence, (4.2) holds for all $x \in \mathbb{S}_n^\circ$, and we have proved the convergence for all $x \in \mathbb{S}_n^-$. The error estimate for the scale function can be obtained from similar calculations, which are omitted here. □

   Proof of Proposition 3: For $x \in \mathbb{S}_n^\circ$, the proof of [55, Proposition 2] shows that

$$|G_n\varphi_k(x) - \mathcal{G}\varphi_k(x)| \le C_1k^4h_n^2.$$

For φ_k the Taylor expansion at x_1 is given by

$$\varphi_k\left(x_1\right) = \varphi_k\left(x_0\right) + \varphi_k'\left(x_0\right)\delta^+x_0 + \frac{1}{2}\varphi_k''\left(x_0\right)\left(\delta^+x_0\right)^2$$

$$+ \frac{1}{6}\varphi_k'''\left(x_0\right)\left(\delta^+x_0\right)^3 + \frac{1}{24}\varphi_k^{(4)}\left(\eta\right)\left(\delta^+x_0\right)^4,$$

for some $\eta \in [x_0, x_1]$. Subtracting $\varphi_k(x_0)$ and dividing by δ^+x_0 yields

$$\nabla^+\varphi_k\left(x_0\right) = \varphi_k'\left(x_0\right) + \frac{1}{2}\varphi_k''\left(x_0\right)\delta^+x_0 + \frac{1}{6}\varphi_k'''\left(x_0\right)\left(\delta^+x_0\right)^2 + \frac{1}{24}\varphi_k^{(4)}\left(\eta\right)\left(\delta^+x_0\right)^3.$$

Further, note that as φ_k is in the domain of the generator, it also satisfies

$$\frac{1}{2}\varphi_k''\left(x_0\right) = \frac{\rho - \mu\left(x_0\right)}{\sigma^2\left(x_0\right)}\varphi_k'\left(x_0\right).$$

Using these results, one obtains

$$|G_n\varphi_k(x_0) - \mathcal{G}\varphi_k(x_0)| = |\rho\beta\nabla^+\varphi_k(x_0) - \rho\varphi_k'(x_0)|$$

$$= \rho\left|(\beta - 1)\varphi_k'(x_0) + \frac{\beta}{2}g''(x_0)\delta^+x_0 + \frac{\beta}{6}\varphi_k'''(x_0)(\delta^+x_0)^2 + \frac{\beta}{24}\varphi_k^{(4)}(\eta)(\delta^+x_0)^3\right|$$

$$= \rho\left|(\beta - 1)\varphi_k'(x_0) + \beta\frac{\rho - \mu(x_0)}{\sigma^2(x_0)}\varphi_k'(x_0)\delta^+x_0 + \frac{\beta}{6}\varphi_k'''(x_0)(\delta^+x_0)^2\right.$$

$$\left. + \frac{\beta}{24}\varphi_k^{(4)}(\eta)(\delta^+x_0)^3\right|$$

$$\leq \begin{cases} C_2\left|\varphi_k'(x_0)\right|\delta^+x_0 + O(h_n^2) \leq C_3\left\|\varphi_k'\right\|_\infty h_n + O(h_n^2) & \text{for Scheme 1,} \\ C_4\frac{|\beta|}{6}\left|\varphi'''(x_0)\right|(\delta^+x_0)^2 + O\left(h_n^3\right) \leq C_5\left\|\varphi_k'''\right\|_\infty h_n^2 + O\left(h_n^3\right) & \text{for Scheme 2,} \end{cases}$$

where the boundedness of β was used, and the particular form of β in Scheme 2 allows the terms involving $\varphi_k'(x_0)$ to cancel. Here the constants C_2, C_3, C_4, $C_5 > 0$ are independent of n and k.

Applying the result from Proposition 1 shows that $\|\varphi_k'\|_\infty \leq C_6 k \leq C_6 k^3$ and $\|\varphi_k'''\|_\infty \leq C_7 k^3$. Thus summarizing the two cases for x_0 and combining them with the result for $x \in \mathbb{S}_n^\circ$ implies

$$\|G_n\varphi_k - \mathcal{G}\varphi_k\|_{n,\infty} \leq \max\{C_1 k^4 h_n^2, C_8 k^3 h_n^\gamma\} \leq C_9 k^4 h_n^\gamma,$$

where C_8, $C_9 > 0$ are independent of n and k, and as always, $\gamma = 1$ for Scheme 1 and $\gamma = 2$ for Scheme 2. Using the fact that $\mathcal{G}\varphi_k = -\lambda_k\varphi_k$ implies

$$\left|\mu_k^n - \lambda_k\right| \leq C_{10} k^4 h_n^\gamma,$$

where $C_{10} > 0$ is a constant independent of k and n, and $\mu_k^n = \arg\min_{\mu \in \Lambda(G_n)}|\mu - \lambda_k|$ with $\Lambda(G_n)$ denoting the set of eigenvalues of $-G_n$. The arguments stated in the proofs of [55, Proposition 2] and [35, Proposition 3.6] still remain valid; hence it can be shown that $\mu_k^n = \lambda_k^n$, and so the claim follows for any $k \leq h_n^{-1/4}$ with sufficiently small h_n. □

Proof of Proposition 4: The main arguments in [55] for the error of eigenfunctions cannot be applied to the problem here, so we use different ideas. Define $\psi_k^n(x) = c\varphi_k^n(x)$ with a constant c such that $\nabla^+\psi_k^n(x_n) = \nabla^+\varphi_k(x_n)$. Furthermore, let $e_k^n(x) = \psi_k^n(x) - \varphi_k(x)$. Then for every $x \in \mathbb{S}_n^\circ$,

$$G_n e_k^n(x) = G_n\left(\psi_k^n(x) - \varphi_k(x)\right)$$

$$= G_n\psi_k^n(x) - \mathcal{G}\varphi_k(x) + (\mathcal{G} - G_n)\varphi_k(x)$$

$$= -\lambda_k^n\psi_k^n(x) + \lambda_k\varphi_k(x) + (\mathcal{G} - G_n)\varphi_k(x)$$

$$= -\lambda_k^n e_k^n(x) - \left(\lambda_k^n - \lambda_k\right)\varphi_k(x) + (\mathcal{G} - G_n)\varphi_k(x).$$

We multiply both sides by $m_n(x)\delta x$ and sum the terms over x from $y \in \mathbb{S}_n^\circ$ to x_n, obtaining

$$\sum_{y \leq x < x_{n+1}} m_n(x)\delta x G_n e_k^n(x)$$

$$= \sum_{y \leq x < x_{n+1}} \delta^- x\nabla^-\left(\frac{1}{s_n(x)}\nabla^+ e_k^n(x)\right) - \sum_{y \leq x < x_{n+1}} k(x)e_k^n(x)m_n(x)\delta x$$

$$= \frac{1}{s_n(x_{n+1})} \nabla^+ e_k^n(x_{n+1}) - \frac{1}{s_n(y^-)} \nabla^+ e_k^n(y^-)$$

$$- \sum_{y \leq x < x_{n+1}} k(x) e_k^n(x) m_n(x) \, \delta x$$

$$= -\frac{1}{s_n(y^-)} \nabla^+ e_k^n(y^-) - \sum_{y \leq x < x_{n+1}} k(x) e_k^n(x) m_n(x) \, \delta x$$

$$= -\lambda_k^n \sum_{y \leq x < x_{n+1}} e_k^n(x) m_n(x) \, \delta x - \left(\lambda_k^n - \lambda_k \right) \sum_{y \leq x < x_{n+1}} \varphi_k(x) m_n(x) \, \delta x$$

$$+ \sum_{y \leq x < x_{n+1}} m_n(x) \, \delta x \, (\mathcal{G} - G_n) \, \varphi_k(x),$$

because $\psi_k^n(x_n) = \varphi_k(x_n)$,

$$\psi_k^n(x_{n+1}) = c \varphi_k^n(x_{n+1}) = \varphi_k(x_{n+1}) = 0,$$

and $\nabla^+ e_k^n(x_n) = 0$. Then

$$\frac{1}{s_n(y^-) \, \delta^+ y^-} e_k^n(y^-) = \frac{1}{s_n(y^-) \, \delta^+ y^-} e_k^n(y) + \sum_{y \leq x < x_{n+1}} \left(k(x) - \lambda_k^n \right) e_k^n(x) m_n(x) \, \delta x$$

$$- \left(\lambda_k^n - \lambda_k \right) \sum_{y \leq x < x_{n+1}} \varphi_k(x) m_n(x) \, \delta x$$

$$+ \sum_{y \leq x < x_{n+1}} m_n(x) \, \delta x \, (\mathcal{G} - G_n) \, \varphi_k(x).$$

Multiplying both sides by $s_n(y^-) \delta^+ y^-$ and taking the absolute value, we get

$$\left| e_k^n(y^-) \right| \leq \left| e_k^n(y) \right| + \left| s_n(y^-) \, \delta^+ y^- \sum_{y \leq x < x_{n+1}} \left(k(x) - \lambda_k^n \right) e_k^n(x) m_n(x) \, \delta x \right|$$

$$+ \left| \left(\lambda_k^n - \lambda_k \right) s_n(y^-) \, \delta^+ y^- \sum_{y \leq x < x_{n+1}} \varphi_k(x) m_n(x) \, \delta x \right|$$

$$+ \left| s_n(y^-) \, \delta^+ y^- \sum_{y \leq x < x_{n+1}} m_n(x) \, \delta x \, (\mathcal{G} - G_n) \, \varphi_k(x) \right|$$

$$\leq \left| e_k^n(y) \right| + C_1 k^2 h_n \sum_{y \leq x < x_{n+1}} \left| e_k^n(x) \right| \delta x \qquad \text{(see (a))}$$

$$+ C_2 k^4 h_n^{\gamma+1} \qquad \text{(see (b))}$$

$$+ C_3 k^4 h_n^{\gamma+1} \qquad \text{(see (c))}$$

$$\leq \left| e_k^n(y) \right| + C_1 k^2 h_n \sum_{y \leq x < x_{n+1}} \left| e_k^n(x) \right| \delta x + C_4 k^4 h_n^{\gamma+1}$$

$$\leq C_5 k^2 h_n \sum_{y \leq x < x_{n+1}} \left| e_k^n(x) \right| \delta x + C_4 k^4 h_n^{\gamma+1}, \qquad \text{(see (d))}$$

where

- (a) holds because $\lambda_k^n \leq Ck^2$ by Lemma (B.3), $m_n(x) \leq C$, $s_n(y^-) \leq C$, and $\delta^+ y^- \leq h_n$;
- (b) holds because $\left| \lambda_k^n - \lambda_k \right| \leq Ck^4 h_n^\gamma$ by (4.4) and

$$
\left| \sum_{y \leq x < x_{n+1}} \varphi_k(x) m_n(x) \, \delta x \right| \leq C h_n \sum_{y \leq x < x_{n+1}} |\varphi_k(x)| \leq C h_n n \, \|\varphi_k\|_\infty \leq C;
$$

- (c) holds because

$$
\left| \sum_{y \leq x < x_{n+1}} m_n(x) \, \delta x \, (\mathcal{G} - G_n) \, \varphi_k(x) \right| \leq \|\mathcal{G}\varphi_k - G_n \varphi_k\|_{n,\infty} \sum_{y \leq x < x_{n+1}} m_n(x) \, \delta x
$$
$$
\leq C \, \|\mathcal{G}\varphi_k - G_n \varphi_k\|_{n,\infty} \, n h_n \leq Ck^4 h_n^\gamma,
$$

  as shown in the proof of Proposition 3, which can be found in the online supplement;

- (d) holds because one can choose C_1 large enough so that $C_1 k^2 h_n \delta x \geq 1$, and the first term can be put into the sum.

The constants $C_1 \ldots, C_5 > 0$ are independent of k, n and x, y. Using the discrete version of Gronwall's inequality and noting that $k \leq h_n^{-1/4}$, we have

$$
\left| e_k^n(y^-) \right| \leq \sum_{y \leq x < x_{n+1}} C_4 k^4 h_n^{\gamma+1} \exp\left(C_5 k^2 h_n \sum_{y \leq x < x_{n+1}} \delta x \right)
$$
$$
\leq C_4 k^4 h_n^{\gamma+1} n \exp\left(C_5 (r - l) \, \delta^{1/2} \right) \leq C_6 k^4 h_n^\gamma.
$$

Note that this inequality also holds for $y = x_{n+1}$ because of the choice of c and ψ_k^n, so that $e_k^n(x_{n+1}) = e_k^n(x_n)$. Furthermore, $C_6 > 0$ is independent of k, n and x, y.

Then we have

$$
\|\varphi_k^n - \varphi_k\|_{n,\infty} = \left\| \frac{\psi_k^n}{\|\psi_k^n\|_{n,2}} - \varphi_k \right\|_{n,\infty} \leq \frac{1}{\|\psi_k^n\|_{n,2}} \|\psi_k^n - \varphi_k\|_{n,\infty} + \left| \frac{1}{\|\psi_k^n\|_{n,2}} - 1 \right| \|\varphi_k\|_\infty
$$
$$
\leq \frac{C_6 k^4 h_n^\gamma}{\|\psi_k^n\|_{n,2}} + C_7 \left| \frac{1}{\|\psi_k^n\|_{n,2}} - 1 \right|,
$$

and furthermore,

$$
\left| 1 - \|\psi_k^n\|_{n,2}^2 \right| = \left| \int_{x_0}^{x_{n+1}} \varphi_k^2(x) M(dx) - \sum_{x \in \mathbb{S}_n^-} \psi_k^n(x)^2 M_n(x) \right|
$$
$$
\leq C_8 \|\varphi_k''\|_\infty h_n^\gamma + \sum_{x \in \mathbb{S}_n^-} \left| \varphi_k(x)^2 - \psi_k^n(x)^2 \right| M_n(x) \leq C_9 k^4 h_n^\gamma,
$$

by making use of Lemma 5 and the fact that

$$\sum_{x \in \mathbb{S}_n^-} \left| \varphi_k(x)^2 - \psi_k^n(x)^2 \right| M_n(x) = \sum_{x \in \mathbb{S}_n^-} \left| e_k^n(x) \right| \left| \varphi_k(x) + \psi_k^n(x) \right| M_n(x)$$

$$\leq \sum_{x \in \mathbb{S}_n^-} \left| e_k^n(x) \right|^2 M_n(x) + 2 \sum_{x \in \mathbb{S}_n^-} \left| e_k^n(x) \right| \left| \varphi_k(x) \right| M_n(x) \leq C_{10} k^4 h_n^\gamma.$$

Putting this result back into the above equation yields

$$\left\| \psi_k^n \right\|_{n,2} \geq \sqrt{1 - C_9 k^4 h_n^\gamma} \geq \sqrt{1 - C_9 \delta^{\gamma - 4/5}},$$

as $k \leq h_n^{-1/5}$. Collecting all results shows that

$$\left\| \varphi_k^n - \varphi_k \right\|_{n,\infty} \leq \frac{C_6 k^4 h_n^\gamma}{\sqrt{1 - C_9 \delta^{\gamma - 4/5}}} + C_7 \left| \frac{1}{\sqrt{1 - C_9 \delta^{\gamma - 4/5}}} - 1 \right| \leq C_{10} k^4 h_n^\gamma,$$

and thus the claim is proved.   □

Proof of Theorem 3: We first take a more detailed look at the approximation of the transition density p_n in the interior of the state space.

Comparing the eigenfunction expansions of p_n and p shows that for $y \in \mathbb{S}_n^\circ$,

$$\left| \frac{1}{m_n(y)} p_n(t, x, y) - \frac{1}{m(y)} p(t, x, y) \right|$$

$$= \left| \sum_{k=1}^n \exp\left(-\lambda_k^n t\right) \varphi_k^n(x) \varphi_k^n(y) - \sum_{k=1}^\infty \exp\left(-\lambda_k t\right) \varphi_k(x) \varphi_k(y) \right|$$

$$\leq \sum_{1 \leq k \leq h_n^{-1/5}} \exp\left(-\lambda_k^n t\right) \left\| \varphi_k^n - \varphi_k \right\|_{n,\infty} \left\| \varphi_k^n \right\|_{n,\infty} + \sum_{1 \leq k \leq h_n^{-1/5}} \exp\left(-\lambda_k^n t\right) \left\| \varphi_k \right\|_\infty \left\| \varphi_k^n - \varphi_k \right\|_{n,\infty}$$

$$+ \sum_{1 \leq k \leq h_n^{-1/5}} \left| \exp\left(-\lambda_k^n t\right) - \exp\left(-\lambda_k t\right) \right| \left\| \varphi_k \right\|_\infty \left\| \varphi \right\|_\infty$$

$$+ \sum_{h_n^{-1/5} < k \leq n} \exp\left(-\lambda_k^n t\right) \left\| \varphi_k^n \right\|_{n,\infty} \left\| \varphi_k^n \right\|_{n,\infty} + \sum_{k > h_n^{-1/5}} \exp\left(-\lambda_k t\right) \left\| \varphi_k \right\|_\infty \left\| \varphi_k \right\|_\infty$$

$$\leq C_1 h_n^\gamma \sum_{1 \leq k \leq h_n^{-1/5}} \exp\left(-C_2 k^2 t\right) \left(k^5 + k^4\right) + C_3 \sum_{1 \leq k \leq h_n^{-1/5}} \left| \exp\left(-\lambda_k^n t\right) - \exp\left(-\lambda_k t\right) \right|$$

$$+ C_4 \sum_{h_n^{-1/5} < k \leq n} \exp\left(-\lambda_k^n t\right) k^2 + C_5 \sum_{k > h_n^{-1/5}} \exp\left(-C_6 k^2 t\right),$$

for positive constants independent of k, n and also x, y. We study the last three terms further: we have

$$C_3 \sum_{1 \leq k \leq h_n^{-1/5}} \left| \exp\left(-\lambda_k^n t\right) - \exp\left(-\lambda_k t\right) \right| \leq C_3 C_7 \sum_{1 \leq k \leq h_n^{-1/5}} \exp\left(-C_8 k^2 t\right) t k^4 h_n^\gamma$$

$$\leq C_9(t) h_n^\gamma,$$

where $C_9(t) = C_3 C_7 \sum_{k=1}^{\infty} \exp\left(-C_8 k^2 t\right) t k^4 < \infty$;

$$C_4 \sum_{h_n^{-1/5} < k \le n} \exp\left(-\lambda_k^n t\right) k^2 \le C_4 n \exp\left(-C_2 h_n^{-2/5} t\right) n^2$$

$$\le C_{10} h_n^2 \exp\left(-C_2 h_n^{-2/5} t\right) n^5$$

$$\le C_{11}(t) h_n^2,$$

where $C_{11}(t) = C_{10} \exp\left(-C_2 h_n^{-2/5} t\right) n^5 < \infty$; and lastly

$$C_5 \sum_{k > h_n^{-1/5}} \exp\left(-C_6 k^2 t\right) \le C_{12} h_n^2 \sum_{k > h_n^{-1/5}} \exp\left(-C_7 k^2 t\right) k^{12} \le C_{13}(t) h_n^2.$$

Summarizing the above results yields

$$\left| \frac{1}{m_n(y)} p_n(t, x, y) - \frac{1}{m(y)} p(t, x, y) \right| \le C_{14}(t) h_n^{\gamma} + C_{15}(t) h_n^2 \le C_t h_n^{\gamma}$$

for some constant $C_t > 0$ depending only on t. Finally, by using the difference between $m_n(x)$ and $m(x)$, derived in (4.2), we obtain

$$p_n(t, x, y) - p(t, x, y) = p(t, x, y) \left(\frac{m_n(y)}{m(y)} - 1 \right) + C_t h_n^{\gamma}$$

$$= p(t, x, y) \frac{\mu(y)}{\sigma^2(y)} \left(\delta^+ y - \delta^- y \right) + C_t h_n^{\gamma}.$$

It can also be shown using the same steps as above that

$$\left| \frac{1}{M_n(y)} P_n(t, x, y) - \frac{1}{M(y)} P(t, x, y) \right| \le C_t h_n^{\gamma},$$

and by (4.1) it holds that

$$P_n(t, x, x_0) - P(t, x, x_0) = P(t, x, x_0) \left(\frac{M_n(x_0)}{M(x_0)} - 1 \right) + C_t h_n^{\gamma}$$

$$= P(t, x, x_0) \frac{\alpha}{\sigma^2(x_0)} \delta x_0 + C_t h_n^{\gamma}.$$

This concludes the proof. $\qquad\square$

Proof of Theorem 4: For $x \in \mathbb{S}_n^-$ we have the following decomposition of the value function:

$$u_n(t, x) - u(t, x) = \sum_{y \in \mathbb{S}_n^-} P_n(t, x, y) f(y) - \int_{x_0}^{x_{n+1}} P(t, x, dy) f(y)$$

$$= P(t, x, x_0) f(x_0) \frac{\alpha}{\sigma^2(x_0)} \delta^+ x_0 + C_t h_n^{\gamma} f(x_0)$$

$$+ \sum_{y \in \mathbb{S}_n^\circ} (p_n(t, x, y) - p(t, x, y)) f(y) \delta y + \sum_{y \in \mathbb{S}_n^\circ} p(t, x, y) f(y) \delta y$$

$$+ \frac{1}{2} p\,(t, x, x_0)\,f\,(x_0)\,\delta^+ x_0 - \frac{1}{2} p\,(t, x, x_0)\,f\,(x_0)\,\delta^+ x_0 - \int_{x_0}^{x_{n+1}} p\,(t, x, y)\,f\,(y)\,dy$$

$$= f\,(x_0)\, \frac{\alpha}{\sigma^2\,(x_0)}\, \delta^+ x_0 M\,(x_0) \sum_{k=1}^{\infty} \exp\,(-\lambda_k t)\,\varphi_k(x)\varphi_k\,(x_0)$$

$$- f\,(x_0)\, \frac{1}{\sigma^2\,(x_0)}\, \delta^+ x_0 \sum_{k=1}^{\infty} \exp\,(-\lambda_k t)\,\varphi_k(x)\varphi_k\,(x_0) + O\left(h_n^\gamma\right) \qquad \text{(see (a))}$$

$$+ \sum_{y \in \mathbb{S}_n^\circ} p\,(t, x, y)\, \frac{\mu\,(y)}{\sigma^2\,(y)}\,\left(\delta^+ y - \delta^- y\right) f\,(y)\,\delta y + O(h_n^2) \qquad \text{(see (b))}$$

$$+ \frac{1}{2} \sum_{y \in \mathbb{S}_n^-} \left(p\,(t, x, y)\,f\,(y) + p\left(t, x, y^+\right) f\left(y^+\right)\right) \delta^+ y - \int_{x_0}^{x_{n+1}} p\,(t, x, y)\,f\,(y)\,dy$$

$$= (\alpha M\,(x_0) - 1)\,O\,(h_n) + O\left(h_n^\gamma\right) + O(h_n^2) \tag{A.5}$$

$$+ \sum_{y \in \mathbb{S}_n^\circ} p\,(t, x, y)\, \frac{\mu\,(y)}{\sigma^2\,(y)}\,\left(\delta^+ y - \delta^- y\right) f\,(y)\,\delta y \tag{A.6}$$

$$+ \frac{1}{2} \sum_{y \in \mathbb{S}_n^-} \left(p\,(t, x, y)\,f\,(y) + p\left(t, x, y^+\right) f\left(y^+\right)\right) \delta^+ y - \int_{x_0}^{x_{n+1}} p\,(t, x, y)\,f\,(y)\,dy, \tag{A.7}$$

where

- (a) holds because

$$p\,(t, x, x_0) = \lim_{y \searrow x_0} p\,(t, x, y) = \frac{2}{\sigma^2\,(x_0)} \sum_{k=1}^{\infty} \exp\,(-\lambda_k t)\,\varphi_k(x)\varphi_k\,(x_0)\,;$$

- (b) holds because of Theorem 3;
- (A.5) holds because

$$\frac{1}{\sigma^2\,(x_0)} \sum_{k=1}^{\infty} \exp\,(-\lambda_k t)\,\varphi_k(x)\varphi_k\,(x_0) \le C_1 \sum_{k=1}^{\infty} \exp\left(-C_2 k^2\right) \le C_3.$$

It can be seen that the approximation error for the value function consists of three parts. The first error is due to the boundary behavior and depends on the scheme. The second error results from the discretization error of the transition kernel, and the last error is the discretization error of the integral. Here we denoted by $O(h_n^\gamma)$ a term that is bounded by $C_t h_n^\gamma$, where the constant C_t is independent of n, x, and y but might depend on t and f.

The first term in (A.5) is of order $O(h_n)$ for Scheme 1 and vanishes for Scheme 2 as $\alpha M(x_0) = \rho \times 1/\rho = 1$. The term in (A.6) is of order $O(h_n^2)$, as can be seen in [55, Equation (23)]. The term in (A.7) is generally of order $O(h_n)$, as seen in [55, Equation (25)]. For call- or put-type payoffs, the term is of order $O(h_n^2)$.

One can also summarize the above cases by using Equation (25) and the proof of Theorem 1 in [55], so that

$$|u_n\,(t, x) - u\,(t, x)| \le p\,(t, x, \xi)\,|f\,(\xi-) - f\,(\xi+)|\,\left|\frac{\xi^- + \xi^+}{2} - \xi\right| + C_t h_n^\gamma,$$

$$|u_n\,(t, x) - u\,(t, x)| \ge p\,(t, x, \xi)\,|f\,(\xi-) - f\,(\xi+)|\,\left|\frac{\xi^- + \xi^+}{2} - \xi\right| - D_t h_n^\gamma,$$

with positive constants $C_t, D_t > 0$ independent of n and x. Taking the maximum on both sides then proves the claim of the theorem. $\qquad\square$

Acknowledgements

References

[1] ALTINISIK, N., KADAKAL, M. AND MUKHTAROV, O. S. (2004). Eigenvalues and eigenfunctions of discontinuous Sturm–Liouville problems with eigenparameter-dependent boundary conditions. *Acta Math. Hung.* **102**, 159–175.

[2] AMIR, M. (1991). Sticky Brownian motion as the strong limit of a sequence of random walks. *Stoch. Process. Appl.* **39**, 221–237.

[3] ANKIRCHNER, S., KRUSE, T. AND URUSOV, M. (2019). *Wasserstein convergence rates for random bit approximations of continuous Markov processes*. Preprint. Available at https://arxiv.org/abs/1903.07880.

[4] BASS, R. F. (2014). A stochastic differential equation with a sticky point. *Electron. J. Prob.* **19**, 1–22.

[5] BONILLA, F. A. AND CUSHMAN, J. H. (2002). Effect of α-stable sorptive waiting times on microbial transport in microflow cells. *Phys. Rev. E* **66**, 031915.

[6] BONILLA, F. A., KLEINFELTER, N. AND CUSHMAN, J. H. (2007). Microfluidic aspects of adhesive microbial dynamics: a numerical exploration of flow-cell geometry, Brownian dynamics, and sticky boundaries. *Adv. Water Resources* **30**, 1680–1695.

[7] BORODIN, A. N. AND SALMINEN, P. (2002). *Handbook of Brownian Motion—Facts and Formulae*, 2nd edn. Birkhäuser, Basel.

[8] BOU-RABEE, N. AND HOLMES-CERFON, M. C. (2020). Sticky Brownian motion and its numerical solution. *SIAM Rev.* **62**, 164–195.

[9] CAI, N., SONG, Y. AND KOU, S. (2015). A general framework for pricing Asian options under Markov processes. *Operat. Res.* **63**, 540–554.

[10] CUI, Z., KIRK, J. L. AND NGUYEN, D. (2017). A general framework for discretely sampled realized variance derivatives in stochastic volatility models with jumps. *Europ. J. Operat. Res.* **262**, 381–400.

[11] CUI, Z., KIRKBY, J. L. AND NGUYEN, D. (2018). A general valuation framework for SABR and stochastic local volatility models. *SIAM J. Financial Math.* **9**, 520–563.

[12] CUI, Z., LEE, C. AND LIU, Y. (2018). Single-transform formulas for pricing Asian options in a general approximation framework under Markov processes. *Europ. J. Operat. Res.* **266**, 1134–1139.

[13] DAVIES, M. AND TRUMAN, A. (1994). Brownian motion with a sticky boundary and point sources in quantum mechanics. *Math. Comput. Modelling* **20**, 173–193.

[14] DAVYDOV, D. AND LINETSKY, V. (2003). Pricing options on scalar diffusions: an eigenfunction expansion approach. *Operat. Res.* **51**, 185–209.

[15] DHILLON, I. (1997). A new $O(n^2)$ algorithm for the symmetric tridiagonal eigenvalue/eigenvector problem. Doctoral Thesis, University of California, Berkeley.

[16] ENGELBERT, H.-J. AND PESKIR, G. (2014). Stochastic differential equations for sticky Brownian motion. *Stochastics* **86**, 993–1021.

[17] ERIKSSON, B. AND PISTORIUS, M. R. (2015). American option valuation under continuous-time Markov chains. *Adv. Appl. Prob.* **47**, 378–401.

[18] FELLER, W. (1952). The parabolic differential equations and the associated semi-groups of transformations. *Ann. Math.* **2**, 468–519.

[19] FENG, L. AND LINETSKY, V. (2008). Pricing options in jump-diffusion models: an extrapolation approach. *Operat. Res.* **56**, 304–325.

[20] GAWEDZKI, K. AND HORVAI, P. (2004). Sticky behavior of fluid particles in the compressible Kraichnan model. *J. Statist. Phys.* **116**, 1247–1300.

[21] GLASSERMAN, P. (2004). *Monte Carlo Methods in Financial Engineering*. Springer, New York.

[22] GRAHAM, C. (1988). The martingale problem with sticky reflection conditions, and a system of particles interacting at the boundary. *Ann. Inst. H. Poincaré Prob. Statist.* **24**, 45–72.

[23] HARRISON, J. M. AND LEMOINE, A. J. (1981). Sticky Brownian motion as the limit of storage processes. *J. Appl. Prob.* **18**, 216–226.

[24] HIGHAM, N. J. (2005). The scaling and squaring method for the matrix exponential revisited. *SIAM J. Matrix Anal. Appl.* **26**, 1179–1193.

[25] IKEDA, N. AND WATANABE, S. (1989). *Stochastic Differential Equations and Diffusion Processes*. North-Holland, Amsterdam.

[26] JIANG, Y., SONG, S. AND WANG, Y. (2019). Some explicit results on one kind of sticky diffusion. *J. Appl. Prob.* **56**, 398–415.

[27] KALDA, J. (2007). Sticky particles in compressible flows: aggregation and Richardson's law. *Phys. Rev. Lett.* **98**, 064501.

[28] KARLIN, S. AND TAYLOR, H. E. (1981). *A Second Course in Stochastic Processes*. Elsevier, New York.

[29] KLOEDEN, P. E. AND PLATEN, E. (1999). *Numerical Solution of Stochastic Differential Equations*. Springer, Berlin.

[30] LI, J., LI, L. AND ZHANG, G. (2017). Pure jump models for pricing and hedging VIX derivatives. *J. Econom. Dynamics Control* **74**, 28–55.

[31] LI, L. AND LINETSKY, V. (2013). Optimal stopping and early exercise: an eigenfunction expansion approach. *Operat. Res.* **61**, 625–643.

[32] LI, L. AND LINETSKY, V. (2014). Time-changed Ornstein–Uhlenbeck processes and their applications in commodity derivative models. *Math. Finance* **24**, 289–330.

[33] LI, L. AND LINETSKY, V. (2015). Discretely monitored first passage problems and barrier options: an eigenfunction expansion approach. *Finance Stoch.* **19**, 941–977.

[34] LI, L. AND ZHANG, G. (2016). Option pricing in some non-Lévy jump models. *SIAM J. Sci. Comput.* **38**, B539–B569.

[35] LI, L. AND ZHANG, G. (2018). Error analysis of finite difference and Markov chain approximations for option pricing. *Math. Finance* **28**, 877–919.

[36] LINETSKY, V. (2008). Spectral methods in derivatives pricing. In Financial Engineering, 1st edn, eds J. R. Birge and V. Linetsky, Elsevier, Amsterdam, pp. 223–299.

[37] LIONS, P. L. AND SZNITMAN, A. S. (1984). Stochastic differential equations with reflecting boundary conditions. *Commun. Pure Appl. Math.* **37**, 511–537.

[38] MCKEAN, H. P. (1956). Elementary solutions for certain parabolic partial differential equations. *Trans. Amer. Math. Soc.* **82**, 519–548.

[39] MEIER, C., LI, L. AND ZHANG, G. (2021). Markov chain approximation of one-dimensional sticky diffusions: supplementary material. Adv. Appl. Prob. Available at http://doi.org/10.1017/apr.2020.65.

[40] MIJATOVIĆ, A. AND PISTORIUS, M. (2013). Continuously monitored barrier options under Markov processes. *Math. Finance* **23**, 1–38.

[41] MUKHTAROV, O. S., KADAKAL, M. AND MUHTAROV, F. S. (2004). On discontinuous Sturm–Liouville problems with transmission conditions. *J. Math. Kyoto Univ.* **44**, 779–798.

[42] NIE, Y. (2017). Term structure modeling at the zero lower bound. Doctoral Thesis, Northwestern University.

[43] NIE, Y. AND LINETSKY, V. (2020). Sticky reflecting Ornstein–Uhlenbeck diffusions and the Vasicek interest rate model with the sticky zero lower bound. *Stoch. Models* **36**, 1–19.

[44] PARASHAR, R. AND CUSHMAN, J. H. (2008). Scaling the fractional advective–dispersive equation for numerical evaluation of microbial dynamics in confined geometries with sticky boundaries. *J. Comput. Phys.* **227**, 6598–6611.

[45] PESKIR, G. (2015). On boundary behaviour of one-dimensional diffusions: from Brown to Feller and beyond. In *William Feller, Selected Papers II*, Springer, Cham, pp. 77–93.

[46] REVUZ, D. AND YOR, M. (2005). *Continuous Martingales and Brownian Motion*. Springer, Berlin.

[47] SKOROKHOD, A. V. (1961). Stochastic equations for diffusion processes in a bounded region. *Theory Prob. Appl.* **6**, 264–274.

[48] SŁOMÍNSKI, L. (1993). On existence, uniqueness and stability of solutions of multidimensional SDE's with reflecting boundary conditions. *Ann. Inst. H. Poincaré Prob. Statist.* **29**, 163–198.

[49] SONG, Y., CAI, N. AND KOU, S. (2019). *A unified framework for regime-switching models*. Preprint. Available at https://ssrn.com/abstract=3310365.

[50] TANAKA, H. (1979). Stochastic differential equations with reflecting boundary condition in convex regions. *Hiroshima Math. J.* **9**, 163–177.

[51] WARREN, J. (1997). Branching processes, the Ray–Knight theorem, and sticky Brownian motion. In *Séminaire de Probabilités XXXI*, eds J. AZÉMA, M. YOR AND M. EMERY, SPRINGER, BERLIN, pp. 1–15.

[52] WATANABE, S. (1971). On stochastic differential equations for multi-dimensional diffusion processes with boundary conditions. *J. Math. Kyoto Univ.* **11**, 169–180.

[53] YAMADA, K. (1994). Reflecting or sticky Markov processes with Lévy generators as the limit of storage processes. *Stoch. Process. Appl.* **52**, 135–164.

[54] ZASLAVSKY, G. M. AND EDELMAN, M. (2005). Polynomial dispersion of trajectories in sticky dynamics. *Phys. Rev. E* **72**, 036204.

[55] ZHANG, G. AND LI, L. (2019). Analysis of Markov chain approximation for option pricing and hedging: grid design and convergence behavior. *Operat. Res.* **67**, 407–427.

[56] ZHANG, G. AND LI, L. (2019). A general method for valuation of drawdown risk under Markovian models. Working paper.